THE JOURNAL OF BIOLOGICAL CHEMISTRY VOL. 287, NO. 36, pp. 30240–30256, August 31, 2012

Mammalian Target of Rapamycin Complex 1 (mTORC1) and 2 (mTORC2) Control the Dendritic Arbor Morphology of Hippocampal Neurons*

Received for publication, April 20, 2012, and in revised form, July 14, 2012 Published, JBC Papers in Press, July 18, 2012, DOI 10.1074/jbc.M112.374405

Malgorzata Urbanska, Agata Gozdz, Lukasz J. Swiech, and Jacek Jaworski[1]

From the International Institute of Molecular and Cell Biology, 02-109, Warsaw, Poland

Background: Neuronal dendrite development is controlled by protein kinases.
Results: Knockdown of Raptor or Rictor, components of mammalian target of rapamycin complex (mTORC1 and -2, respectively) inhibits dendritic growth.
Conclusion: Both mTORC1 and mTORC2 are needed for dendritic growth, with Akt-mTORC1 acting downstream of mTORC2.
Significance: Revealing the mechanism of dendritic growth and mTORC1 and mTORC2 function contributes to the understanding of neuronal plasticity.

Dendrites are the main site of information input into neurons. Their development is a multistep process controlled by mammalian target of rapamycin (mTOR) among other proteins. mTOR is a serine/threonine protein kinase that forms two functionally distinct complexes in mammalian cells: mTORC1 and mTORC2. However, the one that contributes to mammalian neuron development remains unknown. This work used short hairpin RNA against Raptor and Rictor, unique components of mTORC1 and mTORC2, respectively, to dissect mTORC involvement in this process. We provide evidence that both mTOR complexes are crucial for the proper dendritic arbor morphology of hippocampal neurons. These two complexes are required for dendritic development both under basal conditions and upon the induction of mTOR-dependent dendritic growth. We also identified Akt as a downstream effector of mTORC2 needed for proper dendritic arbor morphology, the action of which required mTORC1 and p70S6K1.

Dendrites receive and compute synaptic inputs from other neurons (1). The number of dendrites and their branching patterns are strictly correlated with the function of a particular neuron and geometry of the connections it receives (1). The development of the dendritic arbors of mammalian neurons is driven by several extracellular signals, including neurotrophic factors, cell adhesion molecules, and neuronal activity, which need to be effectively translated to changes in transcription, translation, cytoskeleton dynamics, and membrane trafficking (2, 3). Protein kinases play a key role in this process. We and others previously showed that mammalian target of rapamycin (mTOR)[2] kinase is important for dendritic arbor development (4–8).

mTOR is a serine (Ser)/threonine protein kinase that forms two functionally distinct complexes in mammalian cells: mTORC1 and mTORC2 (9, 10). These complexes share some protein components, but their distinctive activities are defined by their unique components: Raptor, Rictor, and mSin1 (9–11). mTORC1 contains Raptor and is the actual target of rapamycin (9). More specifically, rapamycin forms a tripartite complex with mTOR and the 12-kDa FK506-binding protein (FKBP12) that leads to mTORC1 inhibition (12, 13). mTORC2 contains Rictor and mSin1 and is considered resistant to acute treatment with this drug (Ref. 10 but see Ref. 14). Nevertheless, in several non-neuronal cell types, long term rapamycin application led to mTORC2 inhibition (14). It has been also shown that in non-small-cell lung carcinoma cell lines rapamycin can induce activity of known mTORC2 targets like Akt via activation of phosphatidylinositol 3-kinases (PI3K) pathway most likely due to inhibition of negative feedback loops (15). It should be also noted that rapamycin can have non-mTOR-related effects due to its binding to FKBP12 (16, 17).

mTOR kinase has been repeatedly shown to be crucial for neuronal survival, development, and plasticity (18). The role of particular mTOR complexes has been studied less rigorously in neurons, mostly because of technical reasons. Most extant evidence regarding dendritic arborization has been obtained with the use of rapamycin or short hairpin RNA (shRNA) knockdown of mTOR (4, 5, 7). However, studies of dendritic arbor development required long term (>24 h) rapamycin treatment (5) and, therefore, did not provide clear answers about which mTOR complex plays a pivotal role in the dendritic arbor development of mammalian neurons. In fact, both complexes control cellular processes that are known for their participation in dendritogenesis. For example, studies in yeast and mammalian

* This work was supported by FP7 Grant 223276 (NeuroGSK3), FP7 Grant 229676 (HealthProt), and ERA-NET-NEURON/03/2010 (co-financed by the National Centre for Research and Development). This work was also supported by European Union funds by the European Social Fund (to M. U.).
[1] To whom correspondence should be addressed: 4 Ks. Trojdena St., 02-109 Warsaw, Poland. Tel.: 48-22-597-07-55; Fax: 48-22-597-07-15; E-mail: jaworski@iimcb.gov.pl.

[2] The abbreviations used are: mTOR, mammalian target of rapamycin; mTORC1, mTOR complex1; mTORC2, mTOR complex 2; DIV, days *in vitro*; TNDT, total number of dendritic tips; TDL, total dendritic length; tTS, tetracycline trans-repressor; IF, immunofluorescence.

non-neuronal cells strongly suggest the involvement of mTORC1 in the regulation of myriad cellular processes, including translation and microtubule dynamics. Indeed, proteins that control either the translation or interaction of microtubules with actin have been shown to contribute to mTOR-dependent dendritic growth (5, 8). In contrast, mTORC2 has been implicated in the control of actin dynamics via Rho family small GTPases and in the control of the activity of several kinases (*e.g.* Akt) (10, 19–21). Indeed, RhoA, Rac1, and cdc42 are among the best-characterized regulators of dendritic growth (22–24). We previously showed that active Akt enhances dendritic arborization (5, 8). Nevertheless, the involvement of mTORC2 in the development of mammalian neurons has not been directly demonstrated. Using shRNA-driven knockdown of Raptor and Rictor, unique components of mTORC1 and mTORC2, respectively, this study provided evidence that both mTOR complexes are crucial for the proper dendritic arbor morphology of hippocampal neurons. These two complexes are required for dendritic development both under basal conditions and upon the induction of mTOR-dependent dendritic growth. We also identified Akt as a downstream effector of mTORC2 needed for proper dendritic arbor morphology, the action of which required mTORC1 and S6K1 activity.

EXPERIMENTAL PROCEDURES

Antibodies and Reagents—The following antibodies were obtained from commercial sources: rabbit anti-green fluorescent protein (GFP; Medical and Biological Laboratories, Woburn, MA), mouse anti-GFP, rat anti-HA (Roche Applied Science), mouse anti-β-galactosidase (Promega, Madison, WI), mouse anti-α-tubulin (Sigma), rabbit anti-phospho rpS6 (Ser-235/Ser-236; P-S6), rabbit anti-rpS6, rabbit anti-phospho-Akt (Ser-473; P-Akt), mouse anti-Akt, mouse anti-mTOR, rabbit anti-mTOR (Cell Signaling Technology, Danvers, MA), mouse anti-p110α (BD Transduction Laboratories), mouse anti-Rictor, mouse anti-Raptor (Santa Cruz Biotechnology, Santa Cruz, CA), and rabbit anti-phospho-eIF4B (Ser-422; Signalway Antibody, Pearland, TX). Anti-mouse and anti-rabbit Alexa Fluor 488- or 568-conjugated secondary antibodies and horseradish peroxidase-conjugated anti-rabbit and anti-mouse secondary antibodies were obtained from Invitrogen and Jackson ImmunoResearch (West Grove, PA), respectively. Rapamycin was obtained from Calbiochem. Ku-0063794 was purchased from Chemdea (Ridgewood, NJ). Doxycycline and insulin were obtained from Sigma.

DNA Constructs—The following mammalian expression plasmids have been described previously: pSUPER vector (25), β-actin-GFP, p110CAAX, myr-Akt 4Δ129 (myr-Akt) (5), β-actin-monomeric red fluorescent protein (26), EFα-β-gal (27), pEGFPC2-BIO (28), pRK5 myc-Rictor corrected (Addgene plasmid no. 11367) (10), pRK5 HA-Raptor (Addgene plasmid no. 8513) (9), pTET-tTS, pSuper^{TRE} (29). GFP-Raptor was obtained by subcloning Raptor from pRK5 HA-Raptor to a pEGFPC2-BIO vector in SalI and NotI restriction sites. pRK5-Myc-p70S6K-WT that encodes wild type p70S6K1 was obtained from Dr. Sabatini. The plasmid pRK5-p70S6KT389E that encodes a hyperactive mutant of p70S6K1 was generated by *in vitro* mutagenesis (QuikChange site-directed mutagenesis kit; Stratagene, Santa Clara, CA) of the wild type p70S6K1 using the primers T389E-F (5′-CCAGGTCTTTCTGGGTTTT-GAGTATGTGGCTCCATCTG-3′) and T389E-R (5′-CAG-ATGGAGCCACATACTCAAAACCCAGAAAGACCTGG-3′). pSUPER- and pSUPER^{TRE}-shRaptor#1 and pSUPER- and pSUPER^{TRE}-shRaptor#2 sequences were designed against rat Raptor mRNA (XM_213539) that targeted the following sequences of the coding sequence (CDS): 601–619 (shRaptor#1) and 1910–1928 (shRaptor#2). pSUPER and pSUPER^{TRE}-shRictor#1 and pSUPER- and pSUPER^{TRE}-shRictor#2 sequences were designed against rat Rictor mRNA (XM_226812.6) that targeted the following sequences of the coding sequence (CDS): 1876–1894 (shRictor#1) and 2593–2611 (shRictor#2). As a negative control in the RNA interference (RNAi) experiments, pSUPER plasmid that carried scrambled shRNA was used in addition to an empty plasmid. Scrambled shRNAs were designed based on the original siRNA sequences using the online GeneScript tool. The following sequences were used: 5′-GCACATTATTCG-CTACCTC-3′ (sc-shRaptor#1), 5′-ACCAATACTAATCGA-CTCC-3′ (sc-shRaptor#2), 5′-GCCAATAACGTATGTA-GAT-3′ (sc-shRictor#1), and 5′-ACGGAGAGTAGTTGTA-ATC-3′ (sc-shRictor#2).

Cell Cultures, Transfection, and Drug Treatment—HEK293 cell culture, their transfection, and Western blot analysis were performed as described recently (30). The animals used to obtain neurons for tissue cultures were sacrificed according to a protocol approved by the First Ethical Committee, Warsaw, Poland. Primary rat hippocampal and cortical cultures were prepared from embryonic day 18 (E18) rat brains according to Banker and Goslin (31) with modifications and transfected with Lipofectamine2000 (Invitrogen) as recently described (8, 30). For insulin-induced growth, immediately after transfection, the cells were transferred to a regular culture medium that contained a reduced concentration of B27 (0.2% instead of 2%; Invitrogen). Insulin (400 nM) was added for the first time 4 h after transfection and then every 24 h until cell fixation. In the case of transfection with doxycycline-inducible shRNAs, 1 μg/ml doxycycline was added to the culture medium 24 h post-transfection. For biochemical studies that required the high efficiency transfection of neurons, cortical neurons were transfected on DIV0 using an Amaxa Nucleofector II Device and Amaxa Rat Neuron Nucleofector kit (Lonza, Koln, Germany) according to the adjusted manufacturer's protocol (32).

Immunofluorescence—For the immunofluorescent staining of P-S6 and P-Akt, the neurons were fixed with 4% paraformaldehyde that contained 4% sucrose in phosphate-buffered saline for 10 min at room temperature. Afterward, staining was performed according to the manufacturer's protocol (Cell Signaling Technology). The same protocol was used for the detection of phospho-eIF4B. For the immunodetection of endogenous Raptor and Rictor proteins, the cells were fixed for 10 min with ice-cold 100% methanol and air dried. Staining was then performed according to the manufacturer's protocol (Santa Cruz Biotechnology). The immunostaining of transfected proteins was performed as described previously (8).

Image Acquisition and Analysis—For the analysis of dendritic morphology, cell images were obtained with a Nikon fluorescence microscope, Zeiss LSM5 Exciter, or Zeiss LSM710

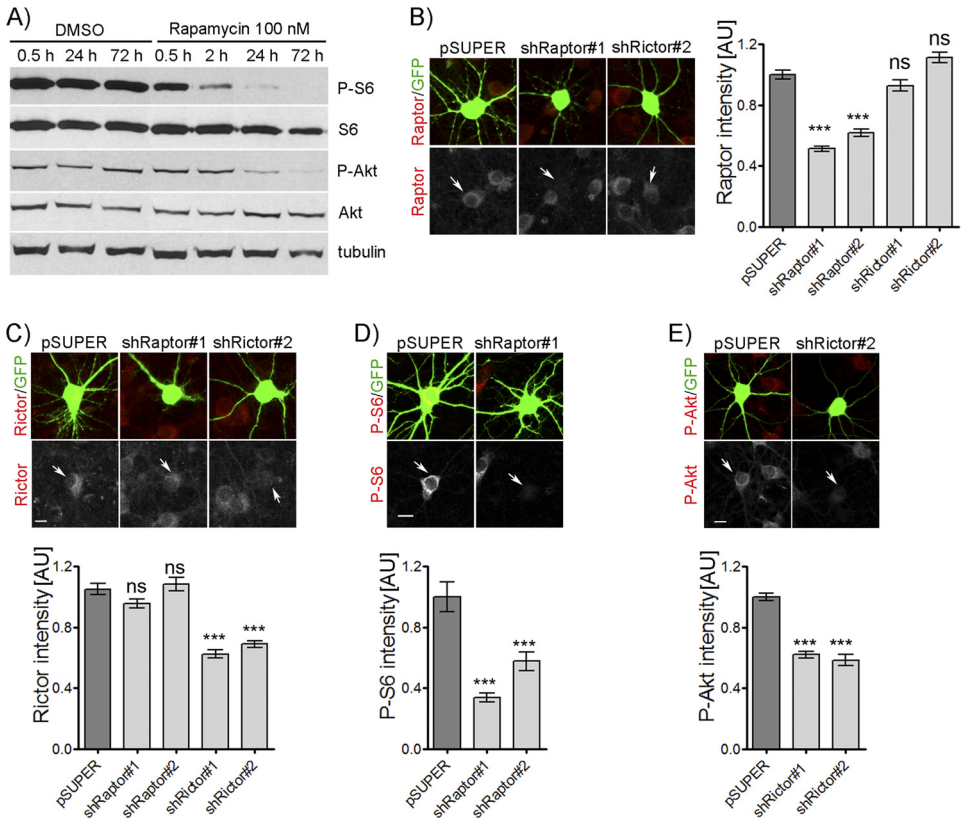

FIGURE 1. **Effects of rapamycin and Raptor and Rictor shRNAs on the activity of mTORC1 and mTORC2, respectively.** *A*, chronic application of rapamycin inhibited the activity of mTORC1 and mTORC2 in cultured hippocampal neurons. Western blot analysis of protein lysates obtained from hippocampal neurons cultured *in vitro* and treated with 100 nM rapamycin on DIV8 for 0.5, 2, 24, and 72 h is shown. Hippocampal neurons cultured *in vitro* were transfected on DIV8 for 3 days with either control pSUPER vector or pSUPER that encoded shRNA against Raptor (*shRaptor#1*, *shRaptor#2*) or Rictor (*shRictor#1*, *shRictor#2*). The cells were co-transfected with a GFP-coding vector for visualization. Afterward, the cells were stained with antibody against endogenous Raptor (*B*) and Rictor (*C*). *AU*, arbitrary units. Additionally, neurons transfected with shRNAs against Raptor were stained for P-S6 (Ser-235/S236) (*D*), whereas those transfected with shRictor were checked for P-Akt (Ser-473) (*E*). Representative images of transfected cells are presented. The efficiency of the shRNAs was estimated by analyzing the average intensity of Raptor (*B*) or Rictor (*C*) immunostaining of transfected cells (*Raptor*: *pSUPER*, $n = 49$; *shRaptor#1*, $n = 37$; *shRaptor#2*, $n = 42$; *shRictor#1*, $n = 40$; shRictor#2, $n = 47$; *Rictor*: pSUPER, $n = 32$; *shRaptor#1*, $n = 32$; *shRaptor#2*, $n = 31$; *shRictor#1*, $n = 32$; *shRictor#2*, $n = 32$). The effects of Raptor and Rictor knockdown on mTORC1 and mTORC2 activity, respectively, were estimated based on the average intensity of P-S6 (*D*) and P-Akt (*E*) immunostaining of the cell soma of transfected cells (*P-S6*: pSUPER, $n = 60$; *shRaptor#1*, $n = 59$; *shRaptor#2*, $n = 60$; *P-Akt*: pSUPER, $n = 73$; *shRictor#1*, $n = 71$; *shRictor#2*, $n = 62$). Cell images were obtained from three independent culture batches. *Error bars* indicate S.E. ***, $p < 0.001$; *ns*, not significant (Mann-Whitney test). *Scale bar* = 10 μm.

NLO with 20× objective. For fluorescence intensity analysis, confocal cell images were obtained with 1024 × 1024 pixel resolution using a Zeiss LSM710 NLO microscope with 20× objective. Each image was a z-series of images, each averaged twice per line. The obtained stack was "flattened" into a single image using a maximum intensity projection. The confocal settings were kept the same for all scans when the fluorescence intensities of immunostaining in neuronal cell somas were compared. Morphometric analysis and quantification were performed as recently described (8, 30). For time-lapse imaging, neurons were imaged with an Olympus ScanR Station microscope with a 20× objective with 1000 × 1000 pixel resolution. Neurons were first imaged 24 h after transfection, and doxycycline was then added. Neurons were then imaged every 24 h for 3 consecutive days. For the analysis, we compared the number of newly added and retracted dendrites between two consecutive imaging sessions.

Immunoprecipitation—For the co-immunoprecipitation experiments, DIV10 cortical neurons nucleofected at DIV0 were harvested in lysis buffer (40 mM HEPES (pH 7.5), 120 mM NaCl, 1 mM EDTA, 0.3% CHAPS, and protease and phosphatase inhibitors). The lysed cells were incubated on ice at 4 °C for 20 min and centrifuged at 14,000 × *g* at 4 °C for 10 min to remove cellular debris. The proteins were then immunoprecipitated with rabbit anti-mTOR conjugated to antibody Sepharose A (Amersham Biosciences). As a negative control, normal rabbit immunoglobulin G (IgG; Sigma) was used. After incubation for 2 h at 4 °C, the resins were washed 4 times with wash buffer (25 mM HEPES (pH 7.4) and 120 mM NaCl) and boiled in SDS-PAGE sample buffer. The samples were analyzed by Western blotting.

Statistical Analysis—The data were obtained from three independent batches of neurons. Exact numbers of cells and culture batches examined for dendritic arbor morphology and fluorescence intensity analyses are provided in the respective figure legends. The statistical analyses were performed using Prism (GraphPad, San Diego, CA) and the Mann-Whitney test.

RESULTS

Knockdown of Either Raptor or Rictor Simplifies Dendritic Arbor Morphology—mTOR kinase has been shown to control dendritic arbor growth in neuronal cultures both *in vitro* and *in vivo* (4–7, 33). However, recent developments in the understanding of the molecular biology of distinct mTOR complexes

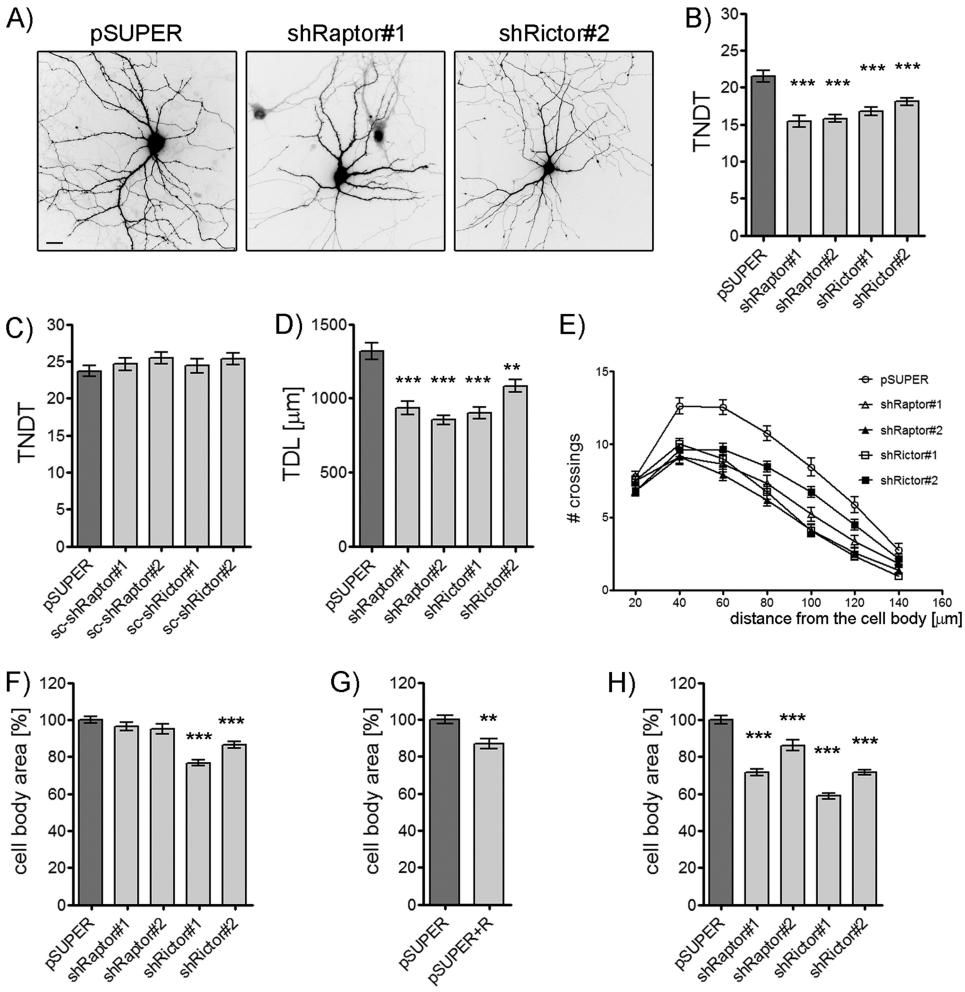

FIGURE 2. **Knockdown of Raptor or Rictor retards the dendritic arborization of hippocampal neurons.** Cultured *in vitro* hippocampal neurons were transfected on DIV8 for 3 days with either control pSUPER vector or pSUPER that encoded shRNA against Raptor (*shRaptor#1*, *shRaptor#2*) or Rictor (*shRictor#1*, *shRictor#2*). In additional control variants, neurons were transfected with vectors that encoded scrambled shRNAs: sc-shRaptor#1, sc-shRaptor#2, sc-shRictor#1, or sc-shRictor#2. The cells were co-transfected with GFP-coding vector for the visualization of neuronal morphology. *A*, shown are representative images of neurons transfected with pSUPER, pSUPER-shRaptor#1, or pSUPER-shRictor#2. *B*, TNDT of hippocampal neurons after Raptor or Rictor knockdown (*pSUPER*, $n = 30$; *shRaptor#1*, $n = 31$; *shRaptor#2*, $n = 36$; *shRictor#1*, $n = 36$; *shRictor#2*, $n = 36$). *C*, shown are TNDT of hippocampal neurons transfected with plasmids that encoded scrambled shRNAs (*pSUPER*: $n = 60$, *sc-shRaptor#1*, $n = 51$; *sc-shRaptor#2*, $n = 51$, *sc-shRictor#1*, $n = 54$; *sc-shRictor#2*, $n = 51$). TDL (*n* as in *B*) (*D*) and Sholl analysis (*n* as in *B*) (*E*) of hippocampal neurons after Raptor or Rictor knockdown is shown. Cell images were obtained from three independent culture batches. *Scale bar* = 20 μm. *F–H*, the effect of rapamycin, Rictor, and Raptor knockdown on cell body area of cultured hippocampal neurons is shown. Cultured *in vitro* hippocampal neurons were transfected on DIV7 for 3 or 5 days with either control pSUPER vector or pSUPER that encoded shRNA against Raptor (*shRaptor#1*, *shRaptor#2*) or Rictor (*shRictor#1*, *shRictor#2*). The cells were co-transfected with a GFP-coding vector for visualization. *F*, shown is average cell body area of neurons transfected for 3 days with control pSUPER vector ($n = 50$) or pSUPER that encoded shRNA against Raptor (*shRaptor#1*, $n = 54$; *shRaptor#2*, $n = 55$) or Rictor (*shRictor#1*, $n = 49$; *shRictor#2*, $n = 53$). *G*, shown is average cell body area of neurons transfected for 3 days with control pSUPER vector treated for 3 days with DMSO ($n = 36$) or 100 nM rapamycin (*R*) ($n = 35$). *H*, shown is average cell body area of neurons transfected for 5 days with control pSUPER vector ($n = 80$) or pSUPER that encoded shRNA against Raptor (*shRaptor#1* $n = 79$; *shRaptor#2*, $n = 76$) or Rictor (*shRictor#1*, $n = 81$; *shRictor#2*, $n = 79$). Cell images were obtained from three independent culture batches. *Error bars* indicate S.E. ***, $p < 0.001$; **, $p < 0.01$ (Mann-Whitney test).

show that previous studies, which mostly utilized chronic rapamycin treatment, could not distinguish which of the complexes is involved in the process of dendritic arbor shaping. Rapamycin was initially believed to be specific for mTORC1 but was later shown to also either block or induce mTORC2 if used chronically (14). What is more, the work done with use of non-small-cell lung carcinoma cell lines showed that chronic rapamycin treatment can induce phosphorylation of known mTORC2 targets (15). Because this issue has not been methodically addressed in neurons, we began our research by determining the effects of long term rapamycin application on the activity of both mTOR complexes (Fig. 1*A*). We treated hippocampal neurons cultured *in vitro* with 100 nM rapamycin for either 0.5 and 2 h or 24 and 72 h to achieve acute and chronic mTOR inhibition, respectively. As shown in Fig. 1*A*, rapamycin at all time points decreased the phosphorylation of rpS6 at Ser-235/236, reflecting decreased mTORC1 activity. Prolonged but not acute rapamycin treatment decreased the phosphorylation of Akt at Ser-473. Such inhibition is a hallmark of mTORC2 activity inhibition (20, 34).

Because long term rapamycin treatment blocked both mTOR complexes, we sought to evaluate the separate roles of mTORC1 and mTORC2 in neuronal development. One way to approach this issue experimentally is to knock down unique components of the mTOR complexes (*i.e.* Raptor (mTORC1) and Rictor (mTORC2)) using RNAi technology. We first

designed a set of specific shRNAs that targeted either Raptor (shRaptor#1 and 2) or Rictor (shRictor#1 and 2) rat mRNA and prepared encoding plasmids based on pSUPER vector. We then tested the effects of Raptor and Rictor knockdown on the proper dendritic arbor morphology of hippocampal neurons. We used hippocampal neurons grown in culture for 8 days *in vitro* (DIV8). We selected this particular time point because intensive dendritogenesis occurs at this time in our prepara-

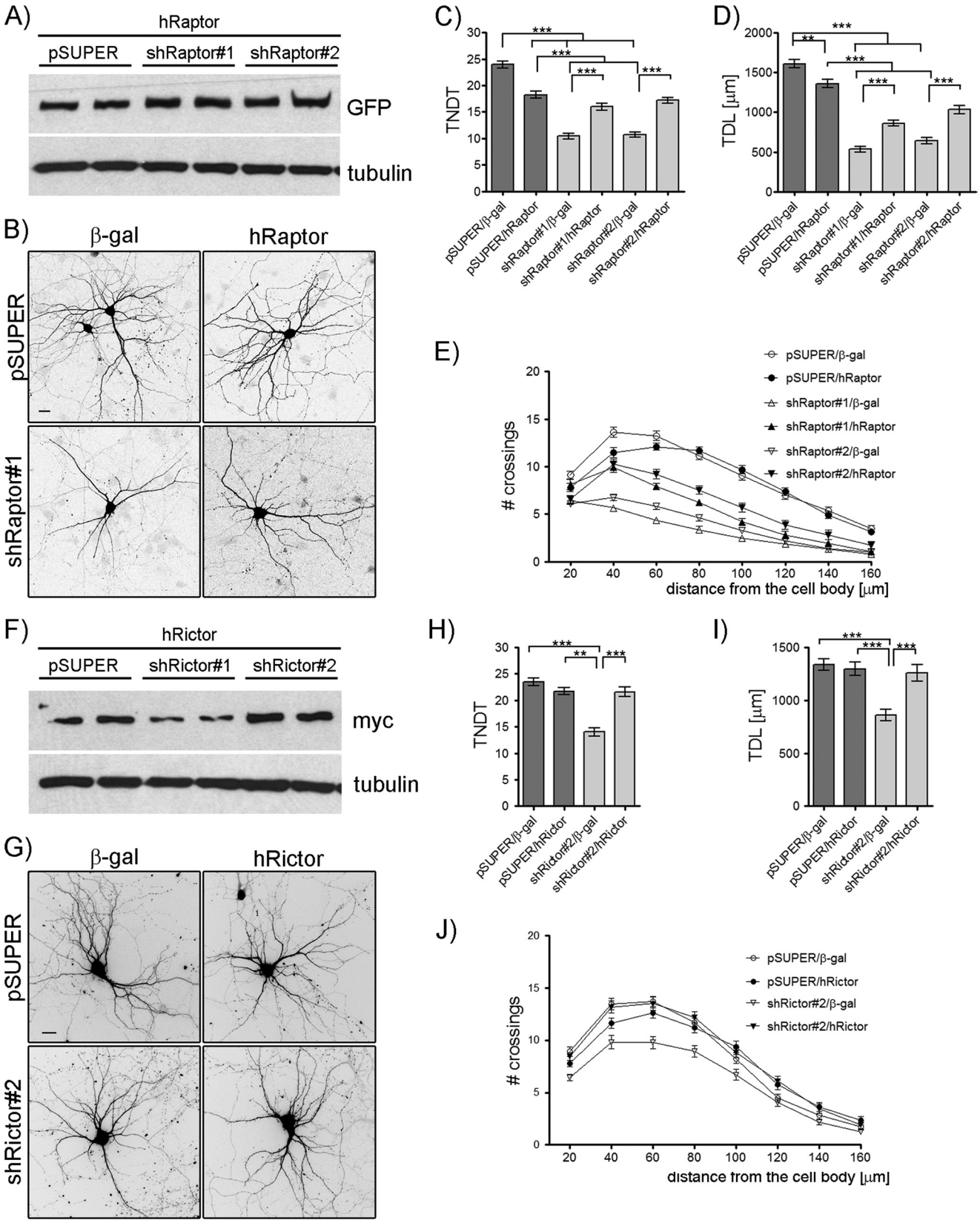

tions. Thus, the neurons were transfected for 3 days with an empty pSUPER plasmid (negative control) or pSUPER that encoded Raptor and Rictor shRNAs, respectively. A plasmid that encoded GFP was added to the transfection mixtures to aid the identification of transfected cells. Endogenous Raptor and Rictor were then detected by immunofluorescence (IF), and the intensities of immunostaining were compared. As shown in Fig. 1*B*, shRNAs directed against Raptor effectively decreased the level of endogenous protein but left Rictor expression intact. Quite to the contrary, Rictor-directed shRNAs strongly decreased the amount of endogenous neuronal Rictor, but Raptor IF was comparable to neighboring, non-transfected cells and pSUPER-transfected controls (Fig. 1*C*). Importantly, we observed a decrease in the levels of P-S6, functionally confirming the decrease in mTORC1 activity, and a decrease in the levels of P-Akt, an mTORC2 activity indicator, for Raptor and Rictor knockdown, respectively (Fig. 1, *D* and *E*).

After establishing the effectiveness of our RNAi tools, we tested the effects of decreased mTORC1 and mTORC2 activity on dendritic arbor development. Thus, we repeated the transfection described above but focused specifically on the morphometric analysis of several parameters that describe dendritic arbor morphology (8, 30). As shown in Fig. 2, the introduction of shRNA against either Raptor or Rictor resulted in a significant simplification of the dendritic arbors of transfected cells. Transfection with pSUPER-shRaptor#1 or pSUPER-shRaptor#2 decreased the total number of dendritic tips (TNDT; 28 and 26%, respectively) compared with neurons transfected with pSUPER (Fig. 2, *A* and *B*). Overexpression of shRictor#1 and shRictor#2 substantially decreased TNDT by 22 and 16%, respectively (Fig. 2, *A* and *B*). We did not observe, however, a similar decrease in TNDT when the cells were transfected with pSUPER that encoded control, scrambled shRNA, designed based on either Raptor (sc-shRaptor#1 and 2), or Rictor (sc-shRictor#1 and 2) shRNA sequence (Fig. 2*C*). In addition to TNDT, we also evaluated the changes in total dendritic length (TDL) evoked by Raptor and Rictor knockdown, respectively. As shown in Fig. 2*D*, TDL significantly decreased under these conditions (by 29, 35, 31, and 18% for shRaptor#1, shRaptor#2, shRictor#1, and shRictor#2, respectively, compared with pSUPER-transfected cells). Finally, to more precisely analyze the pattern of dendritic arborization and assess the coverage of the dendritic fields, we performed a Sholl analysis (35) that measures the number of dendrites that cross circles at various radial distances from the cell soma. In principle, a rightward or upward shift of a Sholl plot corresponds to the increased complexity of the dendritic tree, whereas a leftward and/or downward shift represents shrinkage of the dendritic arbor. The Sholl analysis of Raptor and Rictor knockdown revealed only a downward shift of the plot. At most measured distances, the number of crossings was significantly reduced in neurons that overexpressed shRNAs against either Raptor or Rictor (Fig. 2*E*). However, maximum branching still occurred 40 μm from the center of the cell soma in all cases (pSUPER, 12.6 $\pm$ 0.5; pSUPER-shRaptor#1, 9.1 $\pm$ 0.5; pSUPER-shRaptor#2, 9.0 $\pm$ 0.4; pSUPER-shRictor#1, 10 $\pm$ 0.4; pSUPER-shRictor#2, 9.6 $\pm$ 0.4; $p < 0.001$). We also looked in neurons with either Raptor or Rictor knockdown for a decrease in the cell soma size, which is one of the hallmarks of mTOR inhibition (5). At 3 days post-transfection we did not observe significant changes upon Raptor knockdown and only a slight decrease of cell soma area of cells of Rictor knockdown (Fig. 2*F*). Similarly, a 3-day rapamycin treatment resulted in a slight decrease of cell soma size (Fig. 2*G*). Yet 5 days after transfection, the decrease was evident in cells lacking either Raptor or Rictor (Fig. 2*H*). We suspect that the initial lack of the Raptor shRNAs effects on cell soma size can be explained by the insufficient efficacy of the knockdown. A similar situation was described previously for mTOR shRNA with moderate efficiency, which affected dendritic arbor but not cell soma size upon 3-day overexpression (5).

To further confirm the specificity of the observed Raptor or Rictor knockdown phenotype in neurons, we performed "rescue" experiments that used vectors that encoded human Raptor and Rictor cDNAs that should not be recognized by shRNAs designed against rat sequences. Indeed, as shown in Fig. 3*A*, shRNAs against rat Raptor did not decrease the expression of hRaptor tagged with GFP when co-transfected in HEK293 cells. In the case of Rictor shRNAs, only shRNA#2 did not silence the expression of myc-tagged hRictor in HEK293 cells, consistent with the high homology of shRNA#1-targeted sequences between human and rat (Fig. 3*F*). Hippocampal neurons on DIV8 were then simultaneously transfected for 3 days with a plasmid that encoded either hRaptor (GFP-tagged) or hRictor (myc-tagged) and a suitable shRNA vector. In control variants the cells were transfected with pSUPER and either EFα-β-gal (β-galactosidase-encoding plasmid), hRaptor, or hRictor. Neurons transfected with pSUPER-shRaptor (#1 and #2) or pSUPER-shRictor#2 and EFα-β-gal served as an additional control. In all variants, plasmids that encoded either monomeric red fluorescent protein or GFP were added to the transfection to visualize the morphology of transfected neurons. As shown in Fig. 3, the simultaneous knockdown of endogenous Raptor and overexpression of hRaptor significantly prevented

FIGURE 3. **Morphological effects of Raptor and Rictor silencing are rescued by overexpression of human Raptor and Rictor, respectively.** *A*, when overexpressed in HEK293 cells, GFP-tagged hRaptor was not recognized by co-transfected shRNAs against rat Raptor. *B-E*, and *H-J*, hippocampal neurons cultured *in vitro* were co-transfected on DIV8 for 3 days with EFα-β-gal (control) or hRaptor or hRictor and control pSUPER vector or pSUPER that encoded shRNA against Raptor (*shRaptor#1, shRaptor#2*) or Rictor (*shRictor#2*). *B*, shown are representative images of neurons transfected with either hRaptor or EFα-β-gal and control pSUPER vector or pSUPER that encoded shRNA against Raptor. Neuronal morphology was visualized by co-transfected monomeric red fluorescent protein. Shown is TNDT (*pSUPER/β-gal*, $n = 47$; *shRaptor#1/β-gal*, $n = 51$; *shRaptor#2/β-gal*, $n = 51$, *pSUPER/hRaptor*, $n = 41$; *shRaptor#1/hRaptor*, $n = 40$; *shRaptor#2/hRaptor*, $n = 39$) (*C*), TDL (*n* as in *C*) (*D*), and Sholl analysis (*n* as in *C*) (*E*) of hippocampal neurons after transfection with indicated plasmids. *F*, when overexpressed in HEK293 cells, myc-tagged hRictor was not recognized by co-transfected shRictor#2 against rat Rictor. *G*, shown are representative images of neurons transfected with either hRictor or EFα-β-gal and control pSUPER vector or pSUPER that encoded shRNA against Rictor. Neuronal morphology was visualized by co-transfected GFP. Shown is TNDT (*pSUPER/β-gal*, $n = 52$; *shRictor#2/β-gal*, $n = 52$; *pSUPER/hRictor*, $n = 49$; *shRictor#2/hRictor*, $n = 41$) (*H*), TDL (*n* as in *H*) (*I*), and Sholl analysis (*n* as in *H*) (*J*) of hippocampal neurons after transfection with the indicated plasmids. Cell images were obtained from three independent culture batches. *Error bars* indicate S.E. ***, $p < 0.001$; **, $p < 0.01$ (Mann-Whitney test). *Scale bar* = 20 μm.

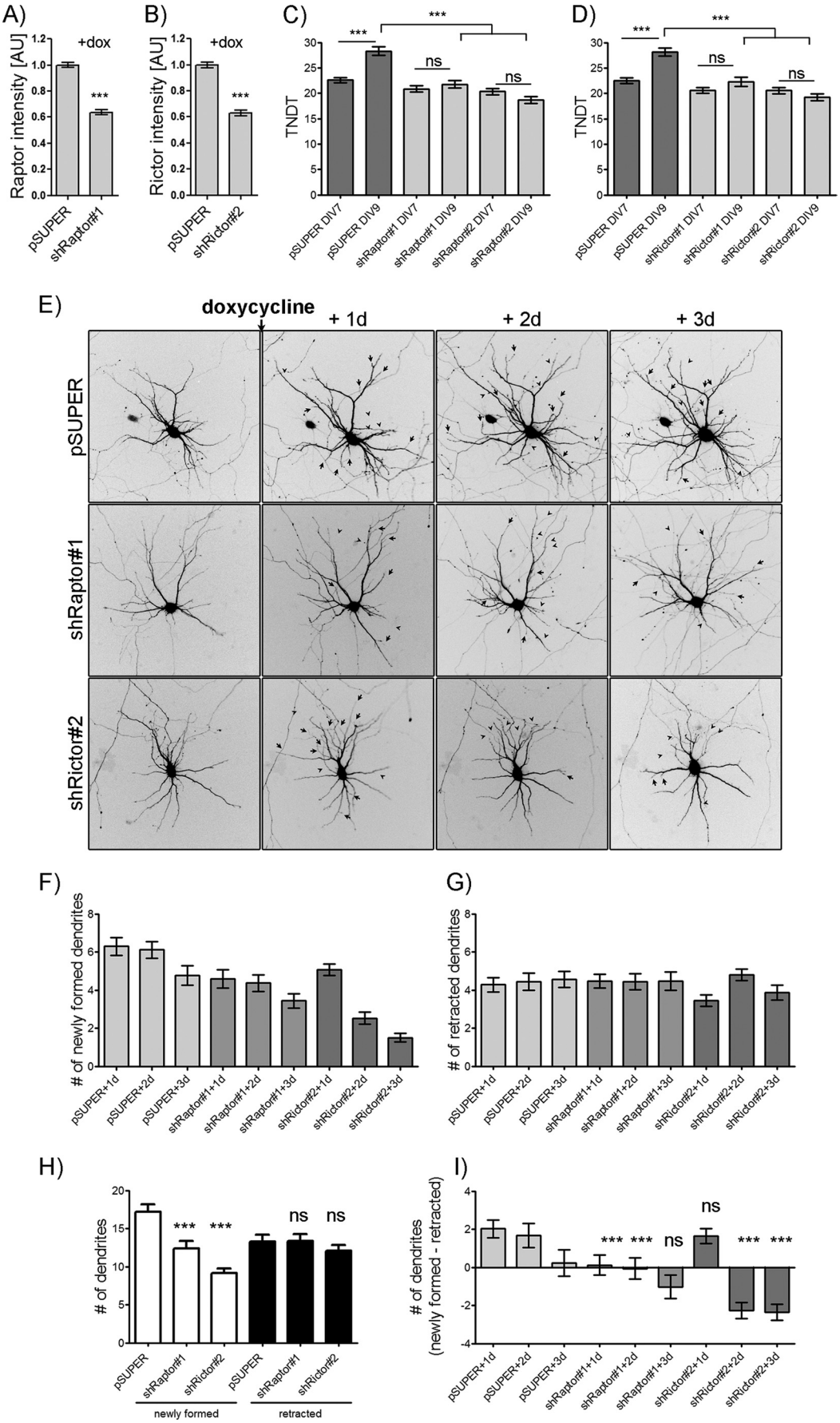
A)
Raptor intensity [AU]
+dox
***
pSUPER
shRaptor#1
B)
Rictor intensity [AU]
+dox
***
pSUPER
shRictor#2
C)
TNDT
***
***
ns
ns
pSUPER DIV7
pSUPER DIV9
shRaptor#1 DIV7
shRaptor#1 DIV9
shRaptor#2 DIV7
shRaptor#2 DIV9
D)
TNDT
***
***
ns
ns
pSUPER DIV7
pSUPER DIV9
shRictor#1 DIV7
shRictor#1 DIV9
shRictor#2 DIV7
shRictor#2 DIV9
E)
doxycycline
+ 1d
+ 2d
+ 3d
pSUPER
shRaptor#1
shRictor#2
F)
# of newly formed dendrites
pSUPER+1d
pSUPER+2d
pSUPER+3d
shRaptor#1+1d
shRaptor#1+2d
shRaptor#1+3d
shRictor#2+1d
shRictor#2+2d
shRictor#2+3d
G)
# of retracted dendrites
pSUPER+1d
pSUPER+2d
pSUPER+3d
shRaptor#1+1d
shRaptor#1+2d
shRaptor#1+3d
shRictor#2+1d
shRictor#2+2d
shRictor#2+3d
H)
# of dendrites
***
***
ns
ns
pSUPER
shRaptor#1
shRictor#2
pSUPER
shRaptor#1
shRictor#2
newly formed
retracted
I)
# of dendrites
(newly formed - retracted)
***
***
ns
ns
***
***
pSUPER+1d
pSUPER+2d
pSUPER+3d
shRaptor#1+1d
shRaptor#1+2d
shRaptor#1+3d
shRictor#2+1d
shRictor#2+2d
shRictor#2+3d

the occurrence of the phenotypic effects of the Raptor knockdown. More specifically, the TNDT of neurons that overexpressed shRaptor and hRaptor was comparable to the TNDT of neurons transfected with hRaptor alone (Fig. 3, *B* and *C*). Considering total dendritic length and the Sholl analysis, the observed rescue was only partial. For pSUPER-shRaptor#1 and pSUPER-shRaptor#2, hRaptor overexpression significantly increased total dendritic length (from 39% for shRaptor#1 to 63% for shRaptor#1/hRaptor and from 47% for shRaptor#2 to 75% for shRaptor#2/hRaptor compared with hRaptor overexpression alone; $p < 0.001$; Fig. 3*D*). The Sholl analysis revealed that at most measured distances, especially those closer to the cell soma, the number of crossings was significantly increased in rescue variants compared with knockdown variants. Nevertheless, the number of crossings did not reach the values of either Raptor- or control pSUPER-transfected cells (Fig. 3*E*). This partial rescue of more complex parameters of the dendritic arbor is consistent with the results obtained by us previously in this type of experiment (8, 30).

With Rictor knockdown, the effect of introducing pSUPER-shRictor#2 on TNDT (35% reduction) was fully restored by the simultaneous overexpression of hRictor protein (Fig. 3, *G* and *H*). Similarly, a high degree of rescue was observed in TDL (from 66% for shRictor#2 to 97% for shRictor#2/hRictor compared with pSUPER/hRictor overexpression; Fig. 3*I*). The Sholl analysis revealed that the number of crossings was significantly higher at most measured distances in rescue variants than in knockdown variants (Fig. 3*J*). Thus, based on these observations, we concluded that both mTORC1 and mTORC2 are needed for proper dendritic arbor morphology formation under basal conditions.

Koike-Kumagai *et al.* (36) used *Drosophila* neurons to show that mTORC1 and mTORC2 do not control the same aspects of dendritic arbor morphology. However, the experiments described above for mammalian neurons showed that knockdown of either Raptor or Rictor simplified the dendritic tree. However, a reduced number of dendrites may result from either the decreased formation of new branches or the accelerated retraction of existing branches. Thus, to distinguish between these two conditions and verify whether mTORCs indeed control dendritic complexity via different means, we utilized doxycycline-induced shRNA expression (8, 37). We assumed that in the case of simple inhibition of dendritic growth, the number of dendrites of the cells fixed immediately and 2 days after knockdown of investigated proteins should be comparable, whereas the dendritic trees of control neurons should show increased complexity. If Raptor or Rictor knockdown results in a combination of growth arrest and accelerated dendritic retraction, then the dendritic trees of neurons fixed at DIV9 should be simplified compared with controls fixed at DIV7. shRaptor (#1 and #2) and shRictor (#1 and #2) were first cloned into a pSUPER^{TRE} plasmid, guaranteeing doxycycline-induced shRNA expression, and co-transfected into DIV6 neurons with a plasmid that encoded tetracycline trans-repressor (tTS). pSUPER^{TRE} was used as a negative control. Doxycycline was added 24 h after transfection, and the cells were fixed either immediately afterward or 48 h later (Fig. 4). As shown in Fig. 4, *A* and *B*, similar to the constitutive approach, the doxycycline-induced expression of Raptor and Rictor shRNA efficiently decreased targeted protein levels. Morphometric analysis of imaged cells revealed that the TNDT of control cells increased significantly for 2 days (Fig. 4, *C* and *D*). However, when the dendritic arbors of DIV9 neurons transfected with shRaptor or shRictor were compared with those of DIV7 cells (control and shRNA-expressing), we observed no increase in TNDT. The analysis of TNDT revealed some leakiness of the doxycycline-induced system. On DIV7 (*i.e.* before adding doxycycline), the TNDT in shRaptor as well as shRictor variants was already slightly decreased. These data suggest that both Raptor and Rictor knockdown reduce dendritic growth rather than induce global dendrite retraction. Reduced dendritic growth may be achieved by several different means (*e.g.* freezing both dendritic growth and retractions or equalizing the formation of new dendrites and retraction of existing ones). To further investigate potential differences in this regard between Raptor and Rictor knockdown, we decided to observe the development of living neurons for 4 consecutive days using time-lapse microscopy. Similar to the experiments described above, we employed inducible shRNAs. As shown in Fig. 4, *E–I*, during the entire 4-day imaging period, control cells formed more new dendrites than retracted existing ones. Thus, despite the steady decrease in dendrite additions, the cells had significantly more dendrites at the end (pSUPER, 24.26 ± 0.90; shRaptor#1, 18.26 ± 0.89; shRictor#2, 15.91 ± 0.78; $p > 0.001$). In contrast, neurons with either Raptor or Rictor knockdown produced fewer new dendrites, whereas the number of retracted dendrites remained relatively stable (Fig. 4, *E–I*). Further inspection of the knockdown effects revealed subtle differences between cells transfected with Raptor and Rictor shRNAs. Raptor knockdown caused rather fast effects. Already 1 day after the induction of

FIGURE 4. **Raptor and Rictor knockdown inhibits dendritic growth under basal culture conditions.** *A* and *B*, doxycycline (*dox*)-induced expression of shRNAs that target Raptor and Rictor diminish the expression of targeted protein. Hippocampal neurons cultured *in vitro* were transfected on DIV6 with a plasmid that encoded tTS and either control pSUPER^{TRE} vector or pSUPER^{TRE} that encoded shRNA against Raptor (*shRaptor#1*, *A*) or Rictor (*shRictor#2*, *B*). *AU*, arbitrary units. The cells were co-transfected with a GFP-coding vector for visualization. On DIV7, doxycycline was added, and cells were fixed on DIV10. Afterward, the cells were stained with antibody against endogenous Raptor or Rictor, and immunofluorescence intensity was quantified (*A*, *pSUPER*^{TRE}, $n = 86$; *shRaptor#1*^{TRE}, $n = 69$; *B*, *pSUPER*^{TRE}, $n = 35$; *shRictor#2*^{TRE}, $n = 37$). Cell images were obtained from three independent culture batches. *Error bars* indicate S.E. ***, $p < 0.001$; *ns*, not significant (Mann-Whitney test). *C*, shown is TNDT of *in vitro*-cultured hippocampal neurons co-transfected on DIV6 with a plasmid that encoded tTS and shRaptor#1^{TRE} ($n = 50$), shRaptor#2^{TRE} ($n = 50$), or pSUPER^{TRE} ($n = 50$) treated with doxycycline on DIV7 and fixed either immediately or on DIV9. *D*, shown is TNDT of *in vitro* cultured hippocampal neurons co-transfected on DIV6 with a plasmid that encoded tTS and shRictor#1^{TRE} (n = 50), shRictor#2^{TRE} (n = 50), or pSuper^{TRE} (n = 50) treated with doxycycline on DIV7 and fixed either immediately or on DIV9. *E*, shown are representative images of cells, the development of which was followed for 3 consecutive days after the induction with doxycycline of either Raptor or Rictor knockdown. *F*, the number of newly added dendrites on each consecutive day (*pSUPER*^{TRE}, $n = 43$; *shRaptor#1*^{TRE}, $n = 34$; *shRictor#2*^{TRE}, $n = 45$) is shown. *G*, shown is the number of retracted dendrites on each consecutive imaging day (*n* as in *F*). *H*, shown is the sum of new additions and retractions during entire experiment. *I*, shown is net change of dendrite number for each consecutive imaging day (*n* as in *F*). Cell images were obtained from three culture batches. *Error bars* indicate S.E. ***, $p < 0.001$; *ns*, not significant (Mann-Whitney test). *Scale bar* = 20 μm.

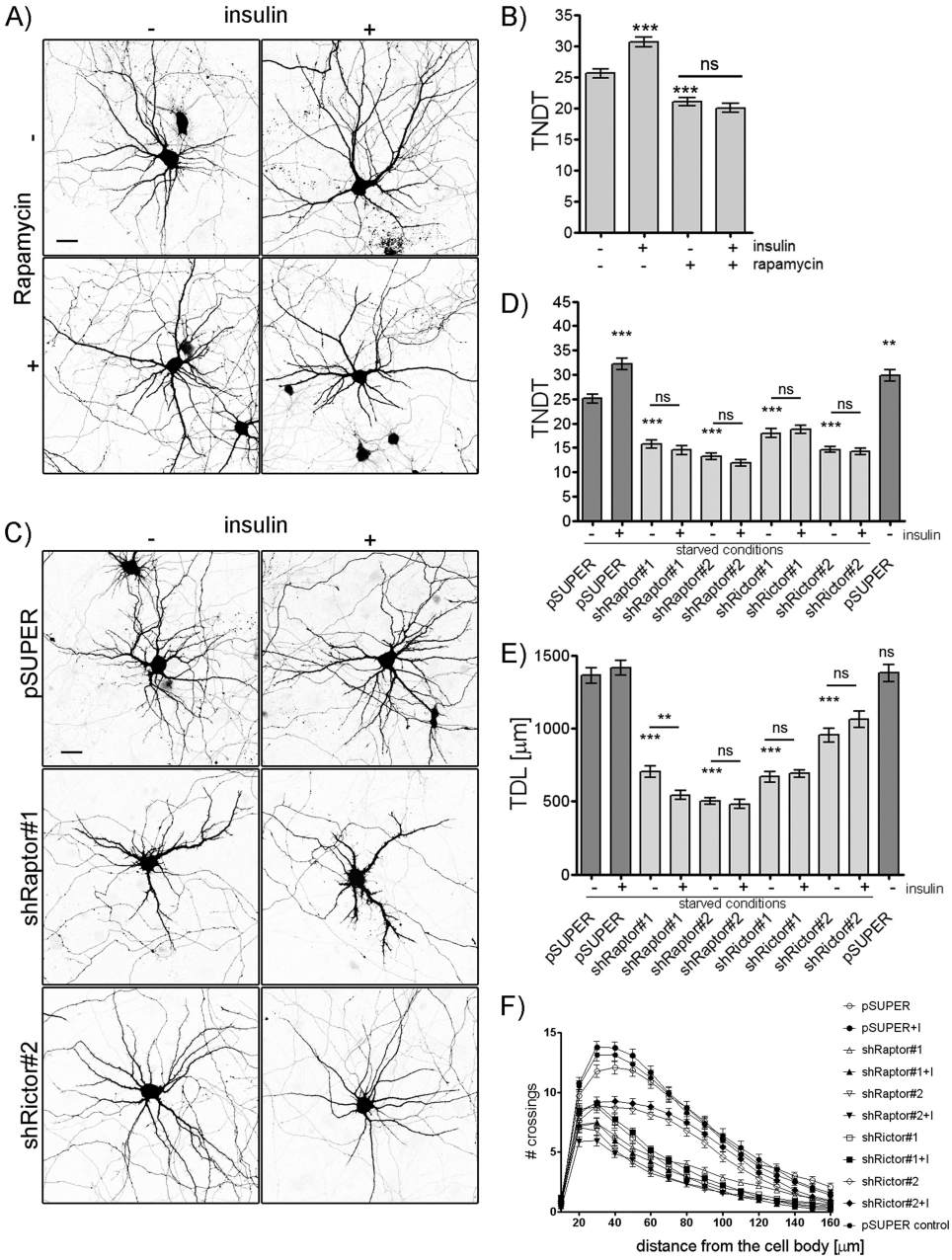

FIGURE 5. **Insulin induces dendritic growth in an mTORC1- and mTORC2-dependent manner.** Shown are representative images (*A*) and analysis of TNDT ($n = 60$ for each experimental group) (*B*) of *in vitro*-cultured hippocampal neurons transfected on DIV8 with GFP and grown for 3 days under conditions of reduced B27 supplementation and in the presence or absence of 100 nM rapamycin. Insulin (400 nM) was added immediately after transfection and then after every 24 h. Shown are representative images (*C*), analysis of TNDT ($n = 52$ for each experimental group) (*D*), analysis of TDL (*n* as in *D*) (*E*), and Sholl analysis (*n* as in *D*) (*F*) of *in vitro*-cultured hippocampal neurons transfected on DIV8 with control pSUPER vector or pSUPER that encoded shRNA against Raptor (*shRaptor#1*, *shRaptor#2*) or Rictor (*shRictor#1*, *shRictor#2*) and grown for 3 days under conditions of reduced B27 supplementation. As an additional control, in one variant the cells were grown under normal B27 conditions. GFP was co-transfected to identify transfected cells and visualize neuronal morphology. Insulin (400 nM) was added immediately after transfection and then after every 24 h. Cell images were obtained from 3 culture batches. *Error bars* indicate S.E. ***, $p < 0.001$; **, $p < 0.01$; *ns*, not significant (Mann-Whitney test). *Scale bar* = 20 μm.

shRNA expression, the number of dendrite additions slightly dropped, matching the number of retractions, and this equilibrium remained stable (Fig. 4, *E–I*). Neurons that lacked Rictor on day 1 exhibited a decrease in the number of additions and retractions, but overall net growth was preserved. However, the next day, a steady and steep decrease in additions occurred, and the cells began to lose dendritic arbor complexity (Fig. 4, *E–I*).

Raptor and Rictor Are Both Required for Insulin- and PI3K-induced Dendritic Growth—The experiments described above showed that both Raptor and Rictor were needed for proper dendritic tree morphology under basal conditions. However, an especially high demand for mTOR activity occurs during the induction of dendritic growth by either growth factors or overexpression of constitutively active PI3K (5). As a pharmacological model of dendritic arbor growth induction, we used prolonged stimulation with 400 nM insulin of neurons grown at a lower concentration of B27 supplementation in the media. B27-starved cells had a lower TNDT than neurons grown under basal conditions, but chronic insulin treatment significantly increased the TNDT of B27-starved cells (Fig. 5, *A* and *B*). This

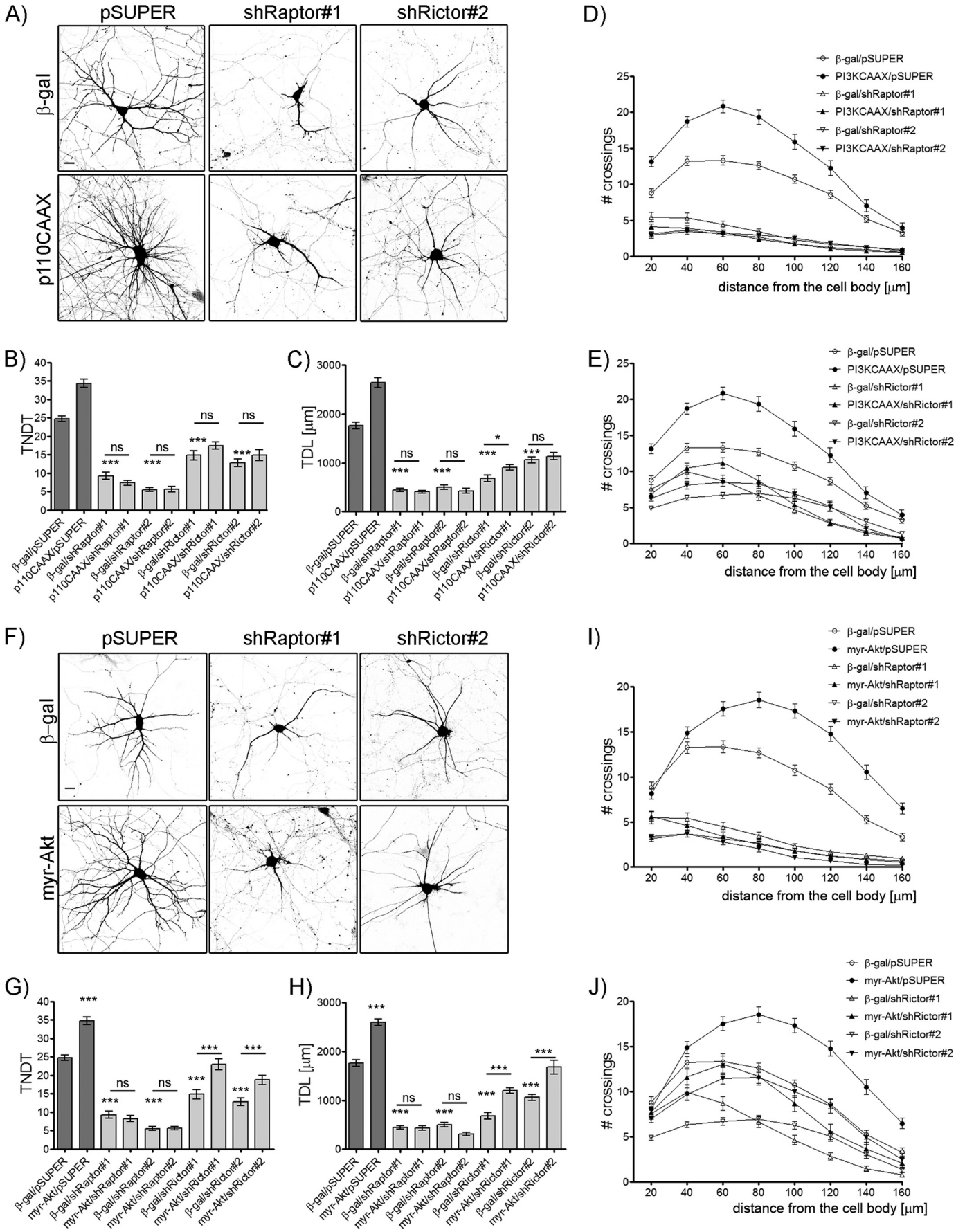
A)
pSUPER
shRaptor#1
shRictor#2
β-gal
p110CAAX
B)
TNDT
C)
TDL [μm]
β-gal/pSUPER
p110CAAX/pSUPER
β-gal/shRaptor#1
p110CAAX/shRaptor#1
β-gal/shRaptor#2
p110CAAX/shRaptor#2
β-gal/shRictor#1
p110CAAX/shRictor#1
β-gal/shRictor#2
p110CAAX/shRictor#2
D)
crossings
distance from the cell body [μm]
PI3KCAAX/pSUPER
PI3KCAAX/shRaptor#1
PI3KCAAX/shRaptor#2
E)
PI3KCAAX/shRictor#1
PI3KCAAX/shRictor#2
F)
myr-Akt
G)
H)
myr-Akt/pSUPER
myr-Akt/shRaptor#1
myr-Akt/shRaptor#2
myr-Akt/shRictor#1
myr-Akt/shRictor#2
I)
J)

increase in TNDT depended on mTOR activity because rapamycin treatment effectively blocked the induction of dendritic arbor growth caused by insulin (Fig. 5, *A* and *B*). In contrast to changes in TNDT, insulin stimulation did not significantly change TDL or the shape of the Sholl plot (Fig. 5, *E* and *F*). To determine whether both mTORCs are essential for insulin-induced growth, we then performed a similar experiment using DIV8 neurons transfected with shRNAs against Raptor and Rictor. Both Raptor and Rictor knockdown impaired insulin-induced dendritic growth, indicating that both complexes are indispensable for the acquisition of proper dendritic morphology when dendritic development is enhanced by trophic stimulation (Fig. 5, *C–F*). These results were further confirmed in our established model of PI3K-induced dendritogenesis. Previous studies suggested that mTORC1 acts as a downstream effector in PI3K-induced growth (5, 7, 8). When we transfected DIV8 neurons with p110CAAX, a constitutively active mutant of PI3K (5, 8), for 5 days, we observed an increase in PI3K protein level in transfected cells (data not shown) and a substantial increase in TNDT and TDL and an upward shift of the Sholl plot compared with control cells transfected with EFα-β-gal (Fig. 6). When p110CAAX was expressed together with shRaptor#1 or shRaptor#2, PI3K-induced growth was completely blocked, confirming that it depends on mTORC1 (Fig. 6, *A–E*). Because we were also interested in whether Rictor, the activity of which is regulated by trophic factors in non-neuronal cells (20), is indispensible for PI3K-induced dendritic growth, we analyzed in parallel the effects of Rictor knockdown in p110CAAX-overexpressing neurons. As shown in Fig. 6, similar to Raptor knockdown, Rictor depletion also inhibited PI3K-induced dendritic growth. More specifically, TNDT and TDL in these cells were similar to transfection with shRictor alone. The Sholl plots of the cells transfected with p110CAAX and shRictor#1 or #2 remained shifted downward. These observations strongly support the involvement of both mTORC1 and mTORC2 in PI3K-induced growth.

Akt Acts Downstream of mTORC2 in Dendritic Arbor Development—Because the mechanisms involved in neurite growth downstream of PI3K and mTORC1 have been steadily revealed (5, 8, 38), we focused our research on defining the proteins that act downstream of mTORC2 in our model of dendritic growth.

We previously showed that Akt acts downstream of PI3K and upstream of mTOR, presumably mTORC1, during hippocampal neuron dendritogenesis (5). However, Akt also serves as a downstream effector of mTORC2 (Fig. 1) (*e.g.* Ref. 20). Thus, we next investigated whether Akt can rescue mTORC2 deficiency during dendritogenesis. We assumed that overexpression of constitutively active Akt (myr-Akt) should efficiently rescue the effects of Rictor knockdown. Although this particular mutant still contains critical Ser-473 that is potentially phosphorylated by mTORC2, it is supposed to act fully independent on mTORC2 (39) and was successfully used previously to reverse the effects of Rictor knock-out in non-neuronal cells (see "Discussion" for details). To test this hypothesis, we transfected DIV8 neurons with plasmids that encoded myr-Akt and shRictor#1, shRictor#2, or pSUPER for 5 days. As an additional control, neurons were transfected with the shRictor-encoding plasmids and EFα-β-gal. myr-Akt was efficiently expressed in neurons, although co-transfection with either Raptor or Rictor shRNAs decreased myr-Akt levels in transfected neurons (data not shown). As shown in Fig. 6, *F–J*, myr-Akt overexpression alone resulted in a substantial increase in TNDT and TDL and an upward shift of the Sholl plot, consistent with our previous observations (5, 8). shRictor alone led to dendritic arbor deterioration. However, when myr-Akt and either of the shRictor-encoding plasmids were overexpressed, the morphology of the dendritic trees of transfected cells had substantially improved, revealed by all three tested parameters, but the restoration of the phenotype was not 100% (Fig. 6, *F–J*). The rescue of myr-Akt was specific for Rictor knockdown because myr-Akt overexpression did not reverse the effects of Raptor knockdown (Fig. 6, *F–J*). In fact, the dendritic arbors of neurons that overexpressed myr-Akt and shRaptor remained equally retarded, similar to those of neurons transfected with shRaptor alone (Fig. 6), supporting the hypothesis that Raptor acts downstream of or parallel to Akt. Thus, based on these results, we conclude that Akt can serve as an important downstream effector of mTORC2 during dendritic growth.

mTORC2 Controls Dendritic Arborization by Acting on mTORC1 and p70S6K1—Our results presented thus far suggest that (i) Akt-induced dendritic growth can rescue mTORC2 knockdown, and (ii) Akt-induced dendritic growth requires Raptor. Moreover, our comparative morphometric analysis revealed that the differences between effects of Raptor and Rictor knockdown are very small. This suggested the possibility that mTORC1 acts downstream of mTORC2 during dendritic growth. If so, then not only should knockdown phenotypes be similar, but also double knockdown would not have a fully additive effect. To test this possibility, we transfected DIV8 neurons with pSUPER or combination of pSUPER-shRaptor#1 and pSUPER-shRictor#2 for 3 days. Additionally, we verified the effects of combined chronic 100 nM rapamycin treatment with

FIGURE 6. **Raptor and Rictor knockdown inhibits dendritic growth induced by constitutively active PI3K, but only Rictor knockdown can be rescued by Akt activation.** *A–E*, hippocampal neurons cultured *in vitro* were co-transfected on DIV8 for 5 days with either EFα-β-gal (control) or p110CAAX and control pSUPER vector or pSUPER that encoded shRNA against Raptor (*shRaptor#1*, *shRaptor#2*) or Rictor (*shRictor#1*, *shRictor#2*). Neuronal morphology was visualized by co-transfected GFP. Shown are representative images of neurons transfected as indicated *A*, TNDT (*B*), TDL (*C*), and Sholl analysis of hippocampal neurons (*D* and *E*) transfected as indicated. *Error bars* indicate S.E. ***, $p < 0.001$; *, $p < 0.05$; *ns*, non significant (Mann-Whitney test). *Scale bar* = 20 μm. *F–J*, hippocampal neurons cultured *in vitro* were co-transfected on DIV8 for 5 days with either EFα-β-gal (control) or myr-Akt and control pSUPER vector or pSUPER-shRaptor#1, pSUPER-shRaptor2, pSUPER-shRictor#1, or pSUPER-shRictor#2. Neuronal morphology was visualized by co-transfected GFP. *F*, representative images of neurons were transfected as indicated. TNDT (*G*), TDL (*H*), and Sholl analysis (*I, J*) of hippocampal neurons were transfected as indicated (*B–J*, *pSUPER/β-gal*, $n = 31$; *shRaptor#1/β-gal*, $n = 36$; *shRaptor#2/β-gal*, $n = 30$; *shRictor#1/β-gal*, $n = 31$; *shRictor#2/β-gal*, $n = 31$; *pSUPER/p110CAAX*, $n = 31$; *shRaptor#1/p110CAAX*, $n = 36$; *shRaptor#2/p110CAAX*, $n = 25$; *shRictor#1/p110CAAX*, $n = 31$; *shRictor#2/p110CAAX*, $n = 31$; *pSUPER/myr-Akt*, $n = 32$; *shRaptor#1/myr-Akt*, $n = 35$; *shRaptor#2/myr-Akt*, $n = 33$; *shRictor#1/myr-Akt*, $n = 34$; *shRictor#2/myr-Akt*, $n = 32$). Cell images were obtained from three independent culture batches. *Error bars* indicate S.E. ***, $p < 0.001$; *ns*, not significant (Mann-Whitney test). *Scale bar* = 20 μm.

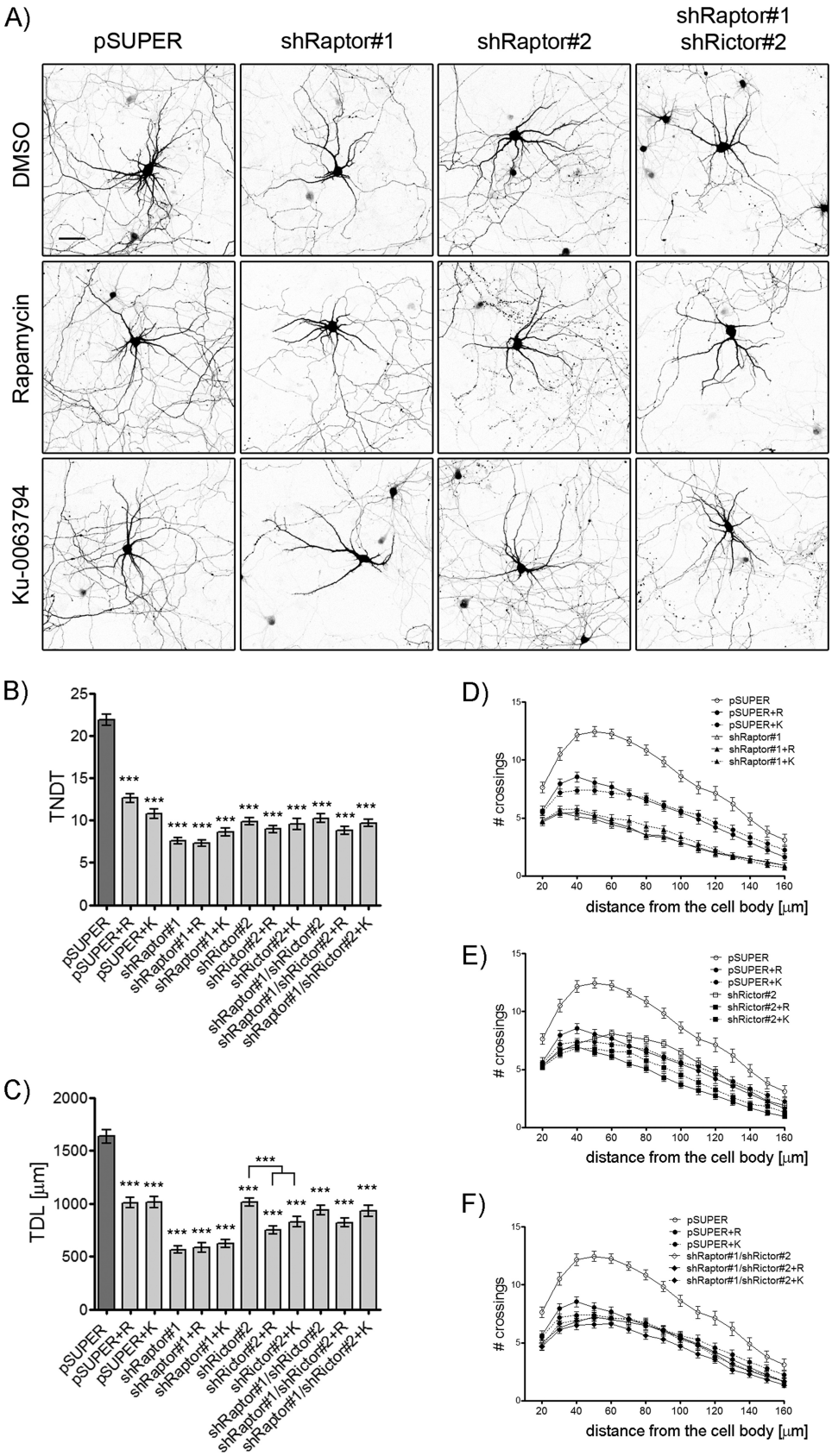
A)
pSUPER
shRaptor#1
shRaptor#2
shRaptor#1
shRictor#2
DMSO
Rapamycin
Ku-0063794
B)
TNDT
pSUPER
pSUPER+R
pSUPER+K
shRaptor#1
shRaptor#1+R
shRaptor#1+K
shRictor#2
shRictor#2+R
shRictor#2+K
shRaptor#1/shRictor#2
shRaptor#1/shRictor#2+R
shRaptor#1/shRictor#2+K
C)
TDL [μm]
D)
crossings
distance from the cell body [μm]
E)
F)

Raptor (sh#1), Rictor (sh#2), or double-knockdown. As shown in Fig. 7, double-knockdown had no additive effect on TNDT. Also, rapamycin treatment of cells with either single or double knockdown did not further decrease TNDT. However, rapamycin slightly enhanced decrease of TDL induced by shRictor#2. Sholl analyses also did not show additive effects. Similar effects were obtained with use of Ku-0063794, an ATP-competitive inhibitor of mTOR that blocks both mTORCs (Fig. 7). Thus, we concluded that the effects of mTORC2 knockdown on dendritic arborization might stem from mTORC1 dysfunction.

Although the analysis of several cell types performed to this point suggested that Rictor knock-out does not affect mTORC1 (40), this issue has not been investigated accurately in neurons. Therefore, we tested the effects of Rictor knockdown on Ser-235/236 phosphorylation in S6 in neurons. Thus, we performed experiments identical to those described in Fig. 1, with the exception that cells transfected with shRNAs against Rictor were stained for P-S6. Additionally, we tested whether Raptor knockdown affects P-Akt IF. As shown in Fig. 8*A*, upon 3-day expression of shRictor#1 or shRictor#2, P-S6 levels significantly dropped compared with controls. Transfection with either of the pSUPER-shRaptor plasmids had no effect on P-Akt levels (Fig. 8*B*). To ensure that indeed our observation was accurate, we used two additional approaches. First, we confirmed that the phosphorylation of eIF4B (S422), another target of mTORC1-p70S6K, was also decreased in neurons upon Rictor knockdown (Fig. 8, *C* and *D*). Second, we used nucleofection of cortical neurons, a highly efficient transfection technique (up to 70% (32)) to obtain independent, biochemical confirmation. As shown in Fig. 8*E*, 10 days after neuron nucleofection (DIV0 + 10), Rictor and Raptor shRNAs effectively knocked down the expression of Rictor and Raptor, respectively. As expected, Raptor knockdown decreased P-S6 but not P-Akt levels. Both Rictor shRNAs resulted in a decrease in P-Akt. However, consistent with the IF data, we observed a substantial decrease in P-S6 levels. At this stage we also verified whether Rictor knockdown affects the integrity of mTORC1, which could explain defects in the phosphorylation of mTORC1-p70S6K substrates independently of Akt dysfunction. To achieve this, mTOR was immunoprecipitated from neurons nucleofected with shRictor#1 or shRictor#2 and probed for Raptor binding. These experiments, however, did not reveal any significant changes in the binding of Raptor to mTOR (Fig. 8*F*).

We then tested whether myr-Akt is capable of restoring P-S6 IF to control levels in neurons with Rictor knockdown. We transfected neurons as described above (Fig. 6). After 3 days we immunofluorescently stained neurons for P-S6. As shown in Fig. 8*G*, the co-transfection of plasmids that encode myr-Akt and pSUPER resulted in an increase in the intensity of P-S6 IF compared with control neurons (pSUPER/EFα-β-gal). In cells transfected with shRictor#1 or #2, P-S6 IF levels were significantly decreased, similar to previous experiments. However, when Rictor knockdown was performed in parallel with myr-Akt overexpression, the levels of P-S6 IF in transfected cells were lower than in myr-Akt/pSUPER-transfected neurons but quite similar to controls (pSUPER/EFα-β-gal). Thus, we concluded that active Akt is able to at least partially restore S6 phosphorylation in Rictor-deficient cells.

p70S6K is a kinase responsible for the phosphorylation of S6 protein in response to Akt-mTORC1 activation. Thus, to test whether mTORC2 controls dendritic arbor growth at least partially via the Akt-mTOR-p70S6K pathway, we determined whether the overexpression of a p70S6KT389E mutant that mimics the phosphorylation of p70S6K1 induced by mTOR can restore P-S6 to control levels in cells transfected with shRNAs against Rictor. Neurons grown for 8 days *in vitro* were transfected with either pSUPER or pSUPER-shRictor#1 or #2 together with p70S6KT389E- or β-gal-encoding vector. As shown in Fig. 8*H*, 3 days post-transfection, P-S6 IF intensity levels in neurons transfected with pSUPER/p70S6KT389E were increased when compared with controls (pSUPER/EFα-β-gal). Additionally, the intensity of P-S6 IF in control cells was similar to cells that overexpressed shRictor and p70S6KT389E as opposed to cells transfected with shRictor and EFα-β-gal. The quantification of TNDT in neurons transfected as described above revealed that p70S6KT389E overexpression, in addition to being able to rescue the intensity of P-S6 IF, was able to return the number of dendrites to the level of control cells (pSUPER/EFα-β-gal transfection; Fig. 8*I*). S6 can also be phosphorylated at Ser-235/236 mTOR-independently because of activation of the ERK kinase signaling pathway. Nevertheless, we did not observe changes in P-ERK levels upon knockdown of Rictor, reflected by both Western blot in cortical neurons and IF in hippocampal cells (data not shown), suggesting that ERK activity was unchanged. Thus, we concluded that the regulation of dendritic arbor development by mTORC2 at least partially relies on Akt-mTORC1-p70S6K1 signaling.

DISCUSSION

Dendritic arbor development depends on mTOR kinase activity, which was repeatedly demonstrated with the use of rapamycin (4, 5, 7). Rapamycin was believed to be a specific mTORC1 inhibitor, but consistent with the results from several non-neuronal cell lines, this study revealed that chronic rapamycin inhibited both mTORCs and led to the conclusion that the previous studies could not determine which mTOR complex is needed for dendritic arbor growth. Therefore, to answer this question, we investigated the effects of shRNA-induced selective knockdown of Raptor and Rictor, unique and critical components of mTORC1 and mTORC2, respectively, on the dendritic arborization of rat hippocampal neurons. We showed that both mTORCs are needed for the proper dendritic morphol-

FIGURE 7. **Simultaneous knockdown of Raptor and Rictor alone or in combination with mTOR inhibitors had no fully additive phenotypic effects on dendritic arborization.** Shown are representative images (*A*) and analysis of TNDT ($n = 39$ for each experimental group) (*B*), TDL (*n* as in *B*) (*C*), and Sholl analysis (*n* as in *B*) (*D–F*) of *in vitro*-cultured hippocampal neurons transfected on DIV8 for 3 days with control pSUPER vector or pSUPER that encoded shRNA against Raptor (*shRaptor#1*) or Rictor (*shRictor#2*) or Raptor and Rictor (*shRaptor#1*, *shRictor#2*). Cells were grown in the absence or presence of 100 nM rapamycin (*R*) or 300 nM Ku-0063794 (*K*). Cell images were obtained from three culture batches. *Error bars* indicate S.E. ***, $p < 0.001$ (Mann-Whitney test). *Scale bar* = 20 μm. Please note that the results presented on *D–F* come from the same three independent experiments but have been split for three graphs for the clarity and convenience of data presentation.

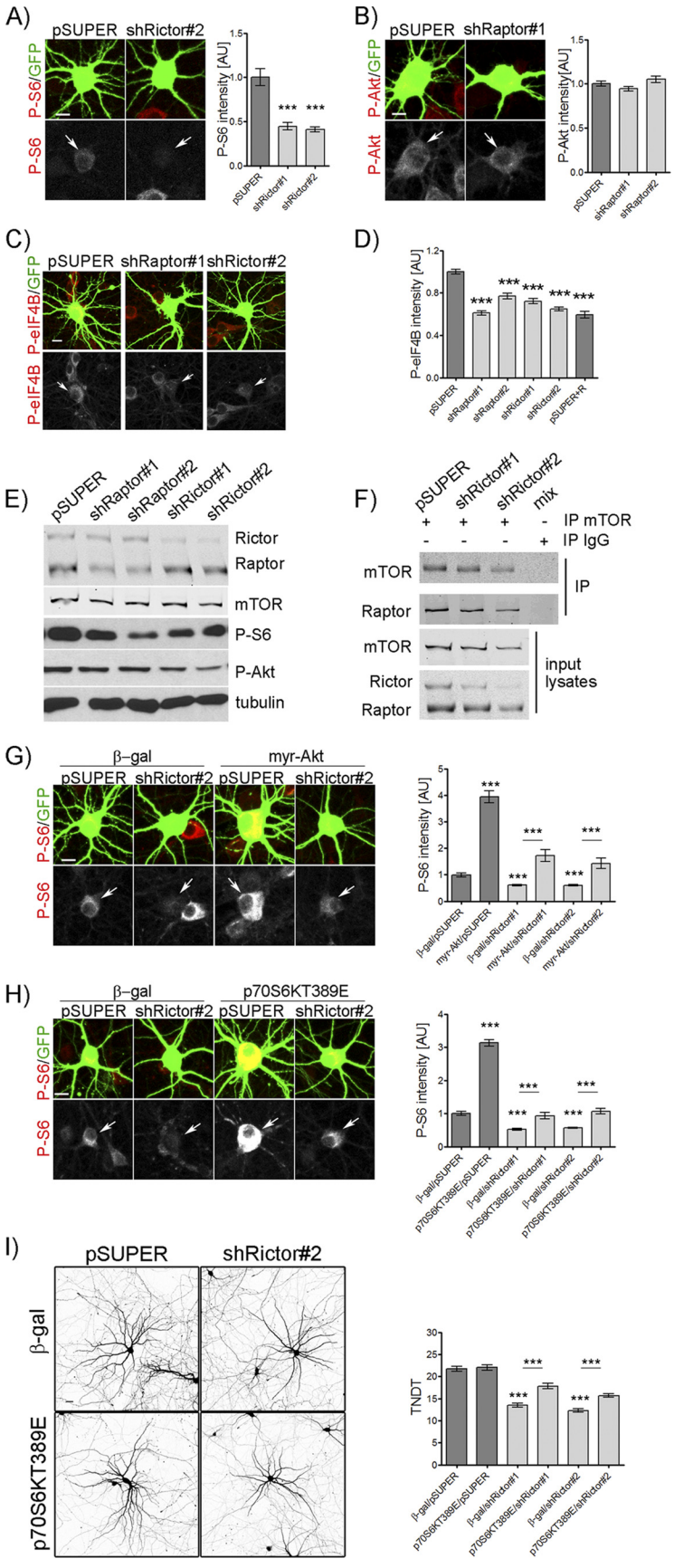
A)
pSUPER shRictor#2
P-S6/GFP
P-S6
P-S6 intensity [AU]
pSUPER
shRictor#1
shRictor#2
B)
pSUPER shRaptor#1
P-Akt/GFP
P-Akt
P-Akt intensity[AU]
pSUPER
shRaptor#1
shRaptor#2
C)
pSUPER shRaptor#1 shRictor#2
P-eIF4B/GFP
P-eIF4B
D)
P-eIF4B intensity [AU]
pSUPER
shRaptor#1
shRaptor#2
shRictor#1
shRictor#2
pSUPER+R
E)
pSUPER
shRaptor#1
shRaptor#2
shRictor#1
shRictor#2
Rictor
Raptor
mTOR
P-S6
P-Akt
tubulin
F)
pSUPER
shRictor#1
shRictor#2
mix
IP mTOR
IP IgG
mTOR
Raptor
IP
mTOR
Rictor
Raptor
input lysates
G)
β–gal
myr-Akt
pSUPER shRictor#2 pSUPER shRictor#2
P-S6/GFP
P-S6
P-S6 intensity [AU]
β-gal/pSUPER
myr-Akt/pSUPER
β-gal/shRictor#1
myr-Akt/shRictor#1
β-gal/shRictor#2
myr-Akt/shRictor#2
H)
β–gal
p70S6KT389E
pSUPER shRictor#2 pSUPER shRictor#2
P-S6/GFP
P-S6
P-S6 intensity [AU]
β-gal/pSUPER
p70S6KT389E/pSUPER
β-gal/shRictor#1
p70S6KT389E/shRictor#1
β-gal/shRictor#2
p70S6KT389E/shRictor#2
I)
pSUPER
shRictor#2
β-gal
p70S6KT389E
TNDT
β-gal/pSUPER
p70S6KT389E/pSUPER
β-gal/shRictor#1
p70S6KT389E/shRictor#1
β-gal/shRictor#2
p70S6KT389E/shRictor#2

ogy of neurons grown under basal culture conditions and treated with insulin or transfected with constitutively active PI3K.

The involvement of mTORC1 in dendritic arbor development, although directly proven herein for mammalian neurons, is not surprising because of previous research on the role of known mTORC1 activators and effectors of dendritic growth (5, 8, 13). This especially refers to dendritic growth induced by the application of growth factors, which are considered canonical activators of mTORC1 signaling (18, 41–43). Brain-derived neurotrophic factor, reelin, and insulin activate PI3K-Akt-mTORC1 and induce the rapamycin-sensitive development of dendritic arbors (5–7) (Figs. 5 and 6). The importance of mTORC1 for dendritic growth is also supported by the analysis of the role of mTORC1 downstream effectors in dendritic growth. For example, Jaworski *et al.* (5) showed that two well characterized mTORC1 targets, p70S6K and 4E-BP1, are indeed crucial for proper dendritic arborization. Recently, another mTORC1 target, cytoplasmic linker protein of 170 kDa (CLIP-170), was shown to regulate PI3K-induced dendritic growth, most likely through its rapamycin-sensitive interaction with IQGAP1 (8).

In this study the use of Rictor shRNA revealed that, in addition to mTORC1, mTORC2 is also indispensible for dendritic development. This observation conflicts with the results of Koike-Kumagai *et al.* (36), who used *Drosophila* class IV dendritic arborization neurons and a mosaic analysis with repressible cell marker technology (44, 45) to show that the inhibition of either Sin1 or Rictor activity autonomously in *Drosophila* dendritic arborization neurons neurons does not significantly affect either dendritic length or the number of dendritic branches. The lack of Rictor alone in neuronal cells affected dendritic tiling, a process of non-redundant coverage of the dendritic fields of homologous neurons (36). This discrepancy can have at least three explanations. First, the difference may arise as a consequence of the different organization and developmental control of vertebrate and invertebrate dendritic arbors (46). Second, mTORC2 may be differentially utilized by neurons that display tiling (*e.g. Drosophila* dendritic arborization neurons and mammalian retinal ganglion cells) and those that do not (*e.g.* hippocampal cells and cortical pyramidal cells). Third, the observed discrepancy might be attributable to several other basic technological differences (*e.g.* shRNA *versus* mosaic analysis with repressible cell marker technology) between our study and that of Koike-Kumagai *et al.* (36). Our hypothesis of the importance of mTORC2 for dendritic growth, based on the results obtained with shRictor, is further corroborated by a similar role of known mTORC2 downstream effectors in dendritic arbor development (*e.g.* Akt, Rho GTPases, and serum- and glucocorticoid-inducible kinase 1 (SGK1)) (5, 7, 23, 47). Thus, our novel finding that Rictor knockdown resulted in the simplification of the dendritic arbors of growing hippocampal neurons potentially unifies previous observations regarding the contributions of three effectors of mTORC2 during this process. However, in this study we provided experimental evidence that supports Akt as a downstream effector of mTORC2 during dendritic growth. Most surprisingly, we found that mTORC1 and p70S6K1 are at least partially responsible for mTORC2-Akt-driven dendritogenesis. These observations require deeper discussions in following aspects; (i) the relationship between myr-Akt and Rictor and (ii) the role of p70S6K1 in the mTORC2-driven regulation of S6 phosphorylation and dendritogenesis.

As previously mentioned, the myr-Akt constitutively active mutant used herein can be subjected to phosphorylation by mTORC2. This is because it still contains a hydrophobic motif domain with Ser-473. One question is how this protein can reverse the effects of Rictor knockdown. One possibility is that membrane targeting caused by a myristoylation signal overrides the need for Ser-473 phosphorylation. No full consensus has been reached regarding this issue (48, 49). Nevertheless, the myr-Akt mutant was shown to effectively reverse the effects of even full Rictor depletion (50–52). Moreover, when the myr-Akt mutant was compared in experiments with phospho-mimicking non-myristoylated Akt mutants, their ability to rescue the phenotypic effects of Rictor knock-out was similar (48). Another potential explanation for mTORC2-independent activation of myr-Akt was provided by work of Warfel *et al.* (39). The authors showed that Ser-473 of Akt mutants lacking pleckstrin homology domain, like our myr-Akt, can be still phosphorylated in the absence of functional mTORC2. In fact it has been postulated that upon a lack of mTORC2, in both cases, *i.e.* superficial membrane targeting and lack of PH domain, Akt

FIGURE 8. **Rictor knockdown effects can be reversed by activation of Akt and p70S6K.** *A* and *B*, hippocampal neurons cultured *in vitro* were transfected on DIV8 for 3 days with either control pSUPER vector or pSUPER that encoded shRNA against Raptor (*shRaptor#1*, *shRaptor#2*) or Rictor (*shRictor#1*, *shRictor#2*). The cells were co-transfected with a GFP-coding vector for visualization. *A*, neurons transfected with shRNAs against Rictor were stained for P-S6 (Ser-235/Ser-236) (*pSUPER*, $n = 63$; *shRictor#1*, $n = 53$; *shRictor#2*, $n = 58$) (*B*), whereas those transfected with shRaptor were checked for P-Akt (Ser-473) (*pSUPER*, $n = 53$; *shRictor#1*, $n = 41$; *shRictor#2*, $n = 44$). *C* and *D*, hippocampal neurons cultured *in vitro* were transfected on DIV8 for 3 days with either control pSUPER vector or pSUPER that encoded shRNA against Raptor (*shRaptor#1*, *shRaptor#2*) or Rictor (*shRictor#1*, *shRictor#2*). Cells were additionally transfected with a GFP-coding vector for visualization. As an additional control, in one variant cells were grown in the presence of 100 nM rapamycin (*R*). Afterward, the cells were stained with antibody against P-eIF4B (Ser-422), and the average intensity of immunostaining of the cell soma of transfected cells was measured (*pSUPER*, $n = 59$; *shRaptor#1*, $n = 55$; *shRaptor#2*, $n = 60$; *shRictor#1*, $n = 60$; *shRictor#2*, $n = 62$, *pSUPER+R*, $n = 61$) (*D*). Cell images were obtained from three culture batches. *Scale bar* = 20 μm. *E* and *F*, cortical neurons at DIV0 were nucleofected with pSUPER vector or pSUPER that encoded shRNA against Raptor (*shRaptor#1*, *shRaptor#2*) or Rictor (*shRictor#1*, *shRictor#2*) for 10 days. Next, the levels of indicated proteins in cell lysates were analyzed (*E*), or immunoprecipitation of mTOR was performed (*F*). Data from one of three experiments are presented. *G*, hippocampal neurons cultured *in vitro* were transfected on DIV8 for 3 days with either EFα-β-gal (control) or myr-Akt and control pSUPER vector or pSUPER that encoded shRNA against Rictor (*shRictor#1*, *shRictor#2*). The cells were co-transfected with a GFP-coding vector for visualization. Cells were stained for P-S6 (Ser-235/S236), and average intensity of cell body immunostaining was measured (*pSUPER/β-gal*, $n = 60$; *shRictor#1/β-gal*, $n = 57$; *shRictor#2/β-gal*, $n = 60$; $n = 31$; *pSUPER/myr-Akt*, $n = 59$; *shRictor#1/myr-Akt*, $n = 59$; *shRictor#2/myr-Akt*, $n = 59$). *H*, hippocampal neurons cultured *in vitro* were transfected on DIV8 for 3 days with either EFα-β-gal (control) or p70S6KT389E and control pSUPER vector or pSUPER that encoded shRNA against Rictor (*shRictor#1*, *shRictor#2*). The cells were co-transfected with a GFP-coding vector for visualization. Cells were stained for P-S6 (Ser-235/Ser-236), and average intensity of cell body immunostaining was measured (*pSUPER/β-gal*, $n = 62$; *shRictor#1/β-gal*, $n = 58$; *shRictor#2/β-gal*, $n = 59$; pSUPER/p70S6KT389E, $n = 62$; *shRictor#1/p70S6KT389E*, $n = 62$; *shRictor#2/p70S6KT389E*, $n = 60$). *Scale bar* = 10 μm. *I*, shown are representative images of neurons transfected as indicated and TNDT (*n* as in *H*). Cell images were obtained from three independent culture batches. *Error bars* indicate S.E. ***, $p < 0.001$ (Mann-Whitney test). *Scale bar* = 20 μm.

phosphorylates itself (39). Thus, although myr-Akt mutant is a good tool to provide evidence for sufficiency of Akt to rescue dendritic arbor simplification upon Rictor knockdown, more experiments are needed in the future with use of additional Akt mutants to fully describe the mechanism of Akt regulation by mTORC2 in neurons.

Our results showed that Rictor knockdown decreased S6 phosphorylation at Ser-235/236. This effect was partially reversed by either myr-Akt or active p70S6K1 overexpression. This suggests that mTORC2 can influence mTORC1 activity in our model. Additionally, such an action is needed for mTORC2 participation in neuronal development. This observation is in contrast to previous observations of non-neuronal cells that lack Rictor, in which although mTORC2 regulated Akt activity, the activity of the mTORC1-p70S6K1 pathway remained intact (40). One obvious possibility is that our Rictor shRNAs have off-target effects that lead to the inhibition of S6 phosphorylation. However, the same constructs, when transfected to RAT2 (*i.e.* a rat embryonic fibroblast line), did not cause such an effect (data not shown). Also, in neurons, both Rictor shRNAs led to a similar effect, although they should principally have non-overlapping off-target effects. Thus, another possibility is that the neurons are different from the other cell types studied thus far. Another possibility is that neurons have additional signaling pathways that would link mTORC2 to p70S6K1. However, if such a case was true, then we would not be able to rescue Rictor knockdown defects on P-S6 by overexpressing Akt.

The data presented herein clearly demonstrate that Rictor knockdown blocked insulin- and PI3K-dependent dendritic growth. However, our different approaches to induce mTORC1- and mTORC2-dependent dendritic growth led to slightly different phenotypes, especially when dendritic arbor morphology was assessed with such a sensitive measure as Sholl analysis. For example, insulin added to B27-starved cells much less effectively induced dendritic growth than the overexpression of p110CAAX or myr-Akt. Moreover, myr-Akt caused more prominent changes in upward and leftward shifts of the Sholl plot than p110CAAX. Differences between pharmacological stimulation and overexpression can be explained in two ways. First, under B27 starvation, insulin might not be sufficient to activate PI3K and Akt to levels that can mimic overexpression conditions. Transfected cells also contain substantially higher levels of PI3K or Akt that cannot be turned off. Second, other B27 components might be needed regardless of the insulin receptor-PI3K-Akt pathway for the induction of dendrite elongation. Differences between the effects of active PI3K and Akt in the Sholl analysis also can be explained in several ways. First, the sizes of the cDNA that encode these two proteins are different. A smaller plasmid (*i.e.* myr-Akt encoding) can be more efficiently transfected, and more protein can be produced. However, more likely is that differences arise because PI3K and Akt targets do not precisely overlap. For example, PI3K activates several small GTPases known to affect dendritic growth, which can lead to a partial reduction of the endogenous effects of Akt. Additionally, cellular levels of endogenous Akt might limit the phenotypic effects of p110CAAX.

Koike-Kumagai *et al.* (36) demonstrated that TORC1 and TORC2 in *Drosophila* play separate roles during dendritic development. TORC1 is important for dendrite extension and branching, and TORC2 controls tiling and the proper separation of dendritic fields between sensory neurons. Our results showed no dramatic differences in this regard between mTORCs, possibly explained by the involvement of mTORC1 in mTORC2-driven dendritic growth. Our data from time-lapse imaging support the existence of subtle distinctions in their contributions to dendritic arborization, which may stem from additional mTORC2 functions.

In conclusion, this study provides deeper insights into trophic factor-, PI3K-, and mTOR-dependent dendritic arborization and new data regarding the effects of rapamycin on neuronal signaling. We showed that PI3K- and insulin-dependent dendritic growth depends on the activation of both mTORC1 and mTORC2, and mTORC1 can act downstream of mTORC2 in developing mammalian neurons. Thus, our study raises an important issue about the interpretation of results obtained with the use of such stimuli or long term rapamycin treatment in studies that focus not only on neuronal development but also neuronal plasticity.

Acknowledgments—We thank Dr. David Sabatini for the pRK5-Myc-p70S6K-WT plasmid. We express our gratitude to Anna Malik for sharing results before publication and Monika Dudek and Marcelina Pieprzyk for help with the experiments and work organization. We thank Drs. Iwona Cymerman and Michal Hetman for commenting on the manuscript.

REFERENCES

1. Stuart, G., Spruston, N., and Häusser, M. (2007) *Dendrites*, 2nd Ed., Oxford University Press, Oxford
2. Jan, Y. N., and Jan, L. Y. (2010) Branching out. Mechanisms of dendritic arborization. *Nat. Rev. Neurosci.* **11,** 316–328
3. Urbanska, M., Blazejczyk, M., and Jaworski, J. (2008) Molecular basis of dendritic arborization. *Acta Neurobiol. Exp.* (*Wars*) **68,** 264–288
4. Chow, D. K., Groszer, M., Pribadi, M., Machniki, M., Carmichael, S. T., Liu, X., and Trachtenberg, J. T. (2009) Laminar and compartmental regulation of dendritic growth in mature cortex. *Nat. Neurosci.* **12,** 116–118
5. Jaworski, J., Spangler, S., Seeburg, D. P., Hoogenraad, C. C., and Sheng, M. (2005) Control of dendritic arborization by thephosphoinositide-3'-kinase-Akt-mammalian target of rapamycin pathway. *J. Neurosci.* **25,** 11300–11312
6. Jossin, Y., and Goffinet, A. M. (2007) Reelin signals through phosphatidylinositol 3-kinase and Akt to control cortical development and through mTor to regulate dendritic growth. *Mol. Cell Biol.* **27,** 7113–7124
7. Kumar, V., Zhang, M. X., Swank, M. W., Kunz, J., and Wu, G. Y. (2005) Regulation of dendritic morphogenesis by Ras-PI3K-Akt-mTOR and Ras-MAPK signaling pathways. *J. Neurosci.* **25,** 11288–11299
8. Swiech, L., Blazejczyk, M., Urbanska, M., Pietruszka, P., Dortland, B. R., Malik, A. R., Wulf, P. S., Hoogenraad, C. C., and Jaworski, J. (2011) CLIP-170 and IQGAP1 cooperatively regulate dendrite morphology. *J. Neurosci.* **31,** 4555–4568
9. Kim, D. H., Sarbassov, D. D., Ali, S. M., King, J. E., Latek, R. R., Erdjument-Bromage, H., Tempst, P., and Sabatini, D. M. (2002) mTOR interacts with raptor to form a nutrient-sensitive complex that signals to the cell growth machinery. *Cell* **110,** 163–175
10. Sarbassov, D. D., Ali, S. M., Kim, D. H., Guertin, D. A., Latek, R. R., Erdjument-Bromage, H., Tempst, P., and Sabatini, D. M. (2004) Rictor, a novel binding partner of mTOR, defines a rapamycin-insensitive and raptor-independent pathway that regulates the cytoskeleton. *Curr. Biol.* **14,** 1296–1302
11. Frias, M. A., Thoreen, C. C., Jaffe, J. D., Schroder, W., Sculley, T., Carr, S. A., and Sabatini, D. M. (2006) mSin1 is necessary for Akt/PKB phosphor-

ylation, and its isoforms define three distinct mTORC2s. *Curr. Biol.* **16,** 1865–1870
12. Sabatini, D. M., Erdjument-Bromage, H., Lui, M., Tempst, P., and Snyder, S. H. (1994) RAFT1. A mammalian protein that binds to FKBP12 in a rapamycin-dependent fashion and is homologous to yeast TORs. *Cell* **78,** 35–43
13. Yip, C. K., Murata, K., Walz, T., Sabatini, D. M., and Kang, S. A. (2010) Structure of the human mTOR complex I and its implications for rapamycin inhibition. *Mol. Cell* **38,** 768–774
14. Sarbassov, D. D., Ali, S. M., Sengupta, S., Sheen, J. H., Hsu, P. P., Bagley, A. F., Markhard, A. L., and Sabatini, D. M. (2006) Prolonged rapamycin treatment inhibits mTORC2 assembly and Akt/PKB. *Mol. Cell* **22,** 159–168
15. Sun, S. Y., Rosenberg, L. M., Wang, X., Zhou, Z., Yue, P., Fu, H., and Khuri, F. R. (2005) Activation of Akt and eIF4E survival pathways by rapamycin-mediated mammalian target of rapamycin inhibition. *Cancer Res.* **65,** 7052–7058
16. Fulceri, R., Giunti, R., Knudsen, J., Leuzzi, R., Kardon, T., and Benedetti, A. (1999) Rapamycin inhibits activation of ryanodine receptors from skeletal muscle by the fatty acyl CoA-acyl CoA-binding protein complex. *Biochem. Biophys. Res. Commun.* **264,** 409–412
17. Kaftan, E., Marks, A. R., and Ehrlich, B. E. (1996) Effects of rapamycin on ryanodine receptor/Ca^{2+} release channels from cardiac muscle. *Circ. Res.* **78,** 990–997
18. Swiech, L., Perycz, M., Malik, A., and Jaworski, J. (2008) Role of mTOR in physiology and pathology of the nervous system. *Biochim. Biophys. Acta* **1784,** 116–132
19. García-Martínez, J. M., and Alessi, D. R. (2008) mTOR complex 2 (mTORC2) controls hydrophobic motif phosphorylation and activation of serum- and glucocorticoid-induced protein kinase 1 (SGK1). *Biochem. J.* **416,** 375–385
20. Sarbassov, D. D., Guertin, D. A., Ali, S. M., and Sabatini, D. M. (2005) Phosphorylation and regulation of Akt/PKB by the rictor-mTOR complex. *Science* **307,** 1098–1101
21. Jacinto, E., Loewith, R., Schmidt, A., Lin, S., Rüegg, M. A., Hall, A., and Hall, M. N. (2004) Mammalian TOR complex 2 controls the actin cytoskeleton and is rapamycin insensitive. *Nat. Cell Biol.* **6,** 1122–1128
22. Li, Z., Van Aelst, L., and Cline, H. T. (2000) Rho GTPases regulate distinct aspects of dendritic arbor growth in *Xenopus* central neurons *in vivo*. *Nat. Neurosci.* **3,** 217–225
23. Nakayama, A. Y., Harms, M. B., and Luo, L. (2000) Small GTPases Rac and Rho in the maintenance of dendritic spines and branches in hippocampal pyramidal neurons *J. Neurosci.* **20,** 5329–5338
24. Threadgill, R., Bobb, K., and Ghosh, A. (1997) Regulation of dendritic growth and remodeling by Rho, Rac, and Cdc42. *Neuron* **19,** 625–634
25. Brummelkamp, T. R., Bernards, R., and Agami, R. (2002) A system for stable expression of short interfering RNAs in mammalian cells. *Science* **296,** 550–553
26. Hoogenraad, C. C., Feliu-Mojer, M. I., Spangler, S. A., Milstein, A. D., Dunah, A. W., Hung, A. Y., and Sheng, M. (2007) Liprinα1 degradation by calcium/calmodulin-dependent protein kinase II regulates LAR receptor-tyrosine phosphatase distribution and dendrite development. *Dev. Cell* **12,** 587–602
27. Konopka, W., Duniec, K., Mioduszewska, B., Proszynski, T., Jaworski, J., and Kaczmarek, L. (2005) hCMV and Tet promoters for inducible gene expression in rat neurons *in vitro* and *in vivo*. *Neurobiol. Dis.* **19,** 283–292
28. de Boer, E., Rodriguez, P., Bonte, E., Krijgsveld, J., Katsantoni, E., Heck, A., Grosveld, F., and Strouboulis, J. (2003) Efficient biotinylation and single-step purification of tagged transcription factors in mammalian cells and transgenic mice. *Proc. Natl. Acad. Sci. U.S.A.* **100,** 7480–7485
29. van de Wetering, M., Oving, I., Muncan, V., Pon Fong, M. T., Brantjes, H., van Leenen, D., Holstege, F. C., Brummelkamp, T. R., Agami, R., and Clevers, H. (2003) Specific inhibition of gene expression using a stably integrated, inducible small-interfering RNA vector. *EMBO Rep.* **4,** 609–615
30. Perycz, M., Urbanska, A. S., Krawczyk, P. S., Parobczak, K., and Jaworski, J. (2011) Zipcode binding protein 1 regulates the development of dendritic arbors in hippocampal neurons. *J. Neurosci.* **31,** 5271–5285
31. Banker, G., and Goslin, K. (1988) Developments in neuronal cell culture. *Nature* **336,** 185–186
32. Swiech, L., Urbanska, M., Macias, M., Skalecka, A., and Jaworski, J. (2012) in *Protein Kinase Technologies, Neuromethods* (Mukai, H., ed) Vol. 68, pp. 291–318, Springer Science+Business Media, New York
33. Brandt, N., Franke, K., Rasin, M. R., Baumgart, J., Vogt, J., Khrulev, S., Hassel, B., Pohl, E. E., Sestan, N., Nitsch, R., and Schumacher, S. (2007) The neural EGF family member CALEB/NGC mediates dendritic tree and spine complexity. *EMBO J.* **26,** 2371–2386
34. Chen, C. H., Shaikenov, T., Peterson, T. R., Aimbetov, R., Bissenbaev, A. K., Lee, S. W., Wu, J., Lin, H. K., and Sarbassov dos, D. (2011) ER stress inhibits mTORC2 and Akt signaling through GSK-3β-mediated phosphorylation of rictor. *Sci. Signal.* **4,** ra10
35. Sholl, D. A. (1953) Dendritic organization in the neurons of the visualand motor cortices of the cat. *J. Anat.* **87,** 387–406
36. Koike-Kumagai, M., Yasunaga, K., Morikawa, R., Kanamori, T., and Emoto, K. (2009) The target of rapamycin complex 2 controls dendritic tiling of *Drosophila* sensory neurons through the Tricornered kinase signalling pathway. *EMBO J.* **28,** 3879–3892
37. Hoogenraad, C. C., Milstein, A. D., Ethell, I. M., Henkemeyer, M., and Sheng, M. (2005) GRIP1 controls dendrite morphogenesis by regulating EphB receptor trafficking. *Nat. Neurosci.* **8,** 906–915
38. Morita, T., and Sobue, K. (2009) Specification of neuronal polarity regulated by local translation of CRMP2 and Tau via the mTOR-p70S6K pathway. *J. Biol. Chem.* **284,** 27734–27745
39. Warfel, N. A., Niederst, M., and Newton, A. C. (2011) Disruption of the interface between the pleckstrin homology (PH) and kinase domains of Akt protein is sufficient for hydrophobic motif site phosphorylation in the absence of mTORC2. *J. Biol. Chem.* **286,** 39122–39129
40. Guertin, D. A., Stevens, D. M., Thoreen, C. C., Burds, A. A., Kalaany, N. Y., Moffat, J., Brown, M., Fitzgerald, K. J., and Sabatini, D. M. (2006) Ablation in mice of the mTORC components raptor, rictor, or mLST8 reveals that mTORC2 is required for signaling to Akt-FOXO and PKCα but not S6K1. *Dev. Cell* **11,** 859–871
41. Harris, T. E., and Lawrence, J. C., Jr. (2003) TOR signaling. *Sci. STKE* **2003,** re15
42. Hay, N., and Sonenberg, N. (2004) Upstream and downstream of mTOR. *Genes Dev.* **18,** 1926–1945
43. Sarbassov, D. D., Ali, S. M., and Sabatini, D. M. (2005) Growing roles for the mTOR pathway. *Curr. Opin. Cell Biol.* **17,** 596–603
44. Luo, L. (2007) Fly MARCM and mouse MADM. Genetic methods of labeling and manipulating single neurons. *Brain Res. Rev.* **55,** 220–227
45. Wu, J. S., and Luo, L. (2006) A protocol for mosaic analysis with a repressible cell marker (MARCM) in *Drosophila*. *Nat. Protoc.* **1,** 2583–2589
46. Parrish, J. Z., Emoto, K., Kim, M. D., and Jan, Y. N. (2007) Mechanisms that regulate establishment, maintenance, and remodeling of dendritic fields. *Annu. Rev. Neurosci.* **30,** 399–423
47. David, S., Stegenga, S. L., Hu, P., Xiong, G., Kerr, E., Becker, K. B., Venkatapathy, S., Warrington, J. A., and Kalb, R. G. (2005) Expression of serum- and glucocorticoid-inducible kinase is regulated in an experience-dependent manner and can cause dendrite growth. *J. Neurosci.* **25,** 7048–7053
48. Hart, J. R., and Vogt, P. K. (2011) Phosphorylation of AKT. A mutational analysis. *Oncotarget* **2,** 467–476
49. Facchinetti, V., Ouyang, W., Wei, H., Soto, N., Lazorchak, A., Gould, C., Lowry, C., Newton, A. C., Mao, Y., Miao, R. Q., Sessa, W. C., Qin, J., Zhang, P., Su, B., and Jacinto, E. (2008) The mammalian target of rapamycin complex 2 controls folding and stability of Akt and protein kinase C. *EMBO J.* **27,** 1932–1943
50. Lee, K., Gudapati, P., Dragovic, S., Spencer, C., Joyce, S., Killeen, N., Magnuson, M. A., and Boothby, M. (2010) Mammalian target of rapamycin protein complex 2 regulates differentiation of Th1 and Th2 cell subsets via distinct signaling pathways. *Immunity* **32,** 743–753
51. Lee, K., Nam, K. T., Cho, S. H., Gudapati, P., Hwang, Y., Park, D. S., Potter, R., Chen, J., Volanakis, E., and Boothby, M. (2012) Vital roles of mTOR complex 2 in Notch-driven thymocyte differentiation and leukemia. *J. Exp. Med.* **209,** 713–728
52. Brown, J., Wang, H., Suttles, J., Graves, D. T., and Martin, M. (2011) Mammalian target of rapamycin complex 2 (mTORC2) negatively regulates Toll-like receptor 4-mediated inflammatory response via FoxO1. *J. Biol. Chem.* **286,** 44295–44305